

Backpropagation Neural Tree

Varun Ojha^{*1} and Giuseppe Nicosia^{2,3}

¹*Department of Computer Science, University of Reading, Reading, UK*

²*Center of System Biology, University of Cambridge, Cambridge, UK*

³*Department of Biomedical & Biotechnological Sciences, University of Catania, Catania, Italy*

Abstract

We propose a novel algorithm called *Backpropagation Neural Tree* (BNeuralT), which is a *stochastic computational dendritic tree*. BNeuralT takes random *repeated inputs* through its leaves and imposes *dendritic nonlinearities* through its internal connections like a biological *dendritic tree* would do. Considering the dendritic-tree like plausible biological properties, BNeuralT is a *single neuron* neural tree model with its internal sub-trees resembling dendritic nonlinearities. BNeuralT algorithm produces an ad hoc *neural tree* which is trained using a stochastic gradient descent optimizer like gradient descent (GD), momentum GD, Nesterov accelerated GD, Adagrad, RMSprop, or Adam. BNeuralT training has two phases, each computed in a depth-first search manner: the *forward pass* computes neural tree's output in a *post-order traversal*, while the error backpropagation during the *backward pass* is performed recursively in a *pre-order traversal*. A BNeuralT model can be considered a *minimal subset* of a neural network (NN), meaning it is a “thinned” NN whose complexity is lower than an ordinary NN. Our algorithm produces high-performing and parsimonious models balancing the complexity with descriptive ability on a wide variety of machine learning problems: classification, regression, and pattern recognition.

Keywords: Stochastic gradient descent; RMSprop; Backpropagation; Minimal Architecture; Neural networks; Neural trees

1 Introduction

Data-driven learning is a hypothesis (trained model) search from a hypothesis-space that fits input data to its target output as good as possible (a low error on test data). A learning algorithm like neural networks (NNs) parameter optimization via backpropagation is the effort to find such a hypothesis (Rumelhart et al., 1986). We propose a new study of ad hoc *neural trees* generation and their optimization via our *recursive backpropagation algorithm* to find such a hypothesis. Hence, we propose a new algorithm called *Backpropagation Neural Tree* (BNeuralT).

*Corresponding Author: Varun Ojha, email: v.k.ojha@reading.ac.uk;
preprint is under review in *Neural Networks*

1 A tree of BNeuralT is like a biological dendritic tree (Travis et al., 2005; Mel, 2016) that processes
2 repeated inputs connected to a single neuron (Beniaguev et al., 2020; Jones and Kording, 2021)
3 through dendritic nonlinearities (London and Häusser, 2005). Structurally, BNeuralT model is a
4 stochastic *computational dendritic tree* that takes random *repeated inputs* through its leaves and
5 imposes *dendritic nonlinearities* through its internal nodes like a biological dendritic tree would
6 do (Travis et al., 2005; Jones and Kording, 2021). Hence, considering the plausible dendritic-
7 tree-like biological properties, BNeuralT is a *single neuron* neural tree model with its internal
8 nodes resembling dendritic nonlinearities.

9 Structurally, BNeuralT, being a tree, is a minimal subset (highly sparse) of a NN whose com-
10 plexity is comparatively low (Poirazi et al., 2003b). This means that a NN with a very high
11 *dropout* [a network regularization technique (Srivastava et al., 2014)] prior to its training can
12 be similar to BNeuralT, except BNeuralT has dedicated paths from input to output as opposed
13 to sparse NN that has shared connections between nodes. Hence, we aim to gauge the perfor-
14 mance of ad hoc *neural trees* trained using *stochastic gradient descent* (SGD) optimizers like
15 gradient descent (GD), momentum gradient descent (MGD) (Qian, 1999), Nesterov accelerated
16 gradient descent (NAG) (Bengio et al., 2013), adaptive gradient (Adagrad) (Dean et al., 2012),
17 root-mean-square gradient propagation (RMSprop) (Tieleman and Hinton, 2012), and adaptive
18 moment estimation (Adam) (Kingma and Ba, 2015).

19 Operationally, an expression-tree with its operator (node) being neural nodes (i.e., an operator
20 is an activation function), edges being neural weights, and leaves being inputs make a neural tree
21 architecture, where the tree’s architecture itself can be optimized (Chen et al., 2005; Schmidt and
22 Lipson, 2009). The tree’s edges (parameters) optimization is straightforward using a gradient-
23 free method (Rios and Sahinidis, 2013; Kennedy and Eberhart, 1995) where the tree is assumed
24 a target function (Ojha et al., 2017). However, its gradient-based optimization is non-trivial,
25 especially because the error-backpropagation through the tree data structure is recursive to
26 traverse. Our proposed BNeuralT algorithm does a two-phase computation of a neural tree in
27 a depth-first search manner: the *forward pass* computes neural tree’s outputs in a *post-order*
28 *traversal*, while the error backpropagation during the *backward pass* is performed recursively in
29 a *pre-order traversal*.

30 We trained ad hoc neural trees in an *online mode* (example-by-example) or a *mini-batch mode*
31 on a variety of learning problems: classification, regression, and pattern recognition. For classi-
32 fication and pattern recognition problems, BNeuralT has its root node’s children (nodes at tree
33 depth one) strictly dedicated to each target class, and the root node decides the winner class on
34 receiving input data. BNeuralT dedicates its root as the output node for a regression problem.

35 We evaluated BNeuralT’s convergence process on six SGD optimizers and analyzed BNeuralT’s
36 complexity against its convergence accuracy. Each training version was compared with a similar
37 training version of a multi-layer perceptron (MLP) algorithm (i.e., an input-hidden-output NN

1 architecture) and classification and regression algorithms such as decision tree (DT) (Breiman
2 et al., 1984), random forest (RF) (Breiman, 2001), single and multi-objective versions of a
3 heterogeneous flexible neural tree (HFNT^S and HFNT^M) (Ojha et al., 2017), multi-output neural
4 tree (MONT) (Ojha and Nicosia, 2020), Gaussian process (GP) (Rasmussen and Williams, 2006),
5 naïve Bayes classifier (NBC) (Mitchell, 1997), and support vector machine (SVM) (Cortes and
6 Vapnik, 1995; Chang and Lin, 2011; Fan et al., 2008). The results on all problems indicate
7 the success of our BNeuralT algorithm that produces high-performing and parsimonious models
8 balancing the complexity and descriptive ability with a minimal training hyperparameters setup.
9 Our contribution is an innovative recursive backpropagation neural tree algorithm that
10 • takes inspiration from biological dendritic trees to solve a wide class of machine learning
11 problems through a single neuron tree-like model performing dendritic nonlinearities
12 through its internal nodes and resembling a highly sparse neural network.
13 • generates low complexity and high accuracy models. Therefore, we have designed a learning
14 system capable of producing minimal and sustainable neural trees that have fewer
15 parameters to produce more compact and, therefore, sustainable neural models able to
16 reduce CPU time and, consequently, CO₂ emissions for machine learning applications.
17 • shows that the sigmoidal dendritic nonlinearity of *any* stochastic ad hoc neural tree structure
18 can solve machine learning problems with high accuracy, and any such structure excels
19 to genetically optimized neural tree structures, NNs, and other learning algorithms.

20 This paper presents relevant related work in Sec. 2. BNeuralT model’s architecture and properties
21 are described in Sec. 3. Secs. 4.1 and 4.2 outline the hyperparameter settings and experiment
22 versions. The performance of BNeuralT on machine learning problems is summarized in Sec. 5
23 and discussed in Sec. 6, followed by conclusions in Sec. 7. Source code of BNeuralT algorithm
24 and pre-trained models are available at <https://github.com/vojha-code/BNeuralT>.

25 **2 Related works**

26 We review the works defining neural tree architectures and training processes. The early definition
27 of neural trees appeared in (Sakar and Mammone, 1993; Sirat and Nadal, 1990), where the
28 tree’s “root-to-leaf” path is represented as a neural network (NN). Such a tree makes its decision
29 through leaf nodes, and its internal nodes are NNs (or neural nodes). Jordan and Jacobs (1994)
30 proposed a hierarchical mixture expert model that performs construction of a binary tree structure
31 where the model hierarchically combines the outputs of expert networks (feed-forward NNs
32 at the terminal) though getting networks (feed-forward NNs at non-terminal) and propagates
33 computation from “leaf-to-root” and where each NN uses the whole input features set.

34 In contrast, our model is purely a single network (tree) structure representation, whereas a

1 hierarchical mixture expert model is a hierarchical combination of several (preferably small)
2 networks. Therefore, unlike hierarchical mixture expert model, our model is a subset of a NN
3 where “leaf-to-root” has a specific information processing path. In fact, considering plausible
4 inspiration from biological computational dendritic tree (Travis et al., 2005; Mel, 2016; Poirazi
5 et al., 2003b), our model behaves as a single neuron model (Jones and Kording, 2021).

6 Our proposed BNeuralT algorithm generates an *m*-ary tree structure stochastically and assigns
7 edge weights randomly. BNeuralT’s each leaf node (terminal node) takes a single input variable
8 from a set of all available variables (data features). Therefore, in a generated tree, some features
9 could remain unused by the model leading to *only* select features responsible for the prediction.
10 Moreover, tree’s each neural node (non-terminal node) takes a weighted summation of its child’s
11 output. Hence, a BNeuralT model potentially performs an *input dimension reduction* and
12 propagates the computation from *leaf to root*.

13 A recent work of Tanno et al. (2019) demonstrates neural tree as an arrangement of convolution
14 layers and linear classifier as a learning model resembling a decision tree-like classifier where the
15 incoming inputs at the nodes are inferred through the so-called router, processed through tree
16 edges (transformers), and classified through leaf (solver) nodes. In contrast, our model takes
17 image pixels as its inputs. A *leaf-to-root* as a neural tree definition appeared in (Zhang et al.,
18 1997; Chen et al., 2005), where the tree’s leaf nodes are designated inputs, internal nodes are
19 neural nodes, and edges are weights. Such types of neural trees have been subjected to structure
20 optimization (Chen et al., 2005; Ojha et al., 2017) and parameter optimization via gradient-free
21 optimization techniques like particle swarm optimization (Chen et al., 2007) and differential
22 evolution (Ojha et al., 2017).

23 Zhang et al. (1997) demonstrated that a neural tree could be evolved as a subset of an MLP.
24 Their effort was to evolve a neural tree using genetic programming and optimize parameters
25 using a genetic algorithm. Lee et al. (2016) focused on implementing pooling layers within
26 a convolutional NN as a tree structure. However, our approach is to generate and train ad
27 hoc neural trees using our proposed recursive backpropagation algorithm. To the best of our
28 knowledge and review, this is the first and novel attempt to generate and train *ad hoc* neural
29 trees using *our recursive error-backpropagation* algorithm. Our motivation is to avoid any prior
30 assumptions on network architecture and complicated hyperparameter settings.

31 Srivastava et al. (2014) proposed dropout technique that suggests randomly dropping neurons
32 from a large NN. This creates “thinned” NN instances during training and prevents a NN
33 from overfitting. Our proposed BNeuralT randomly generates a tree architecture, which can be
34 considered a sparse NN in a similar sense with rather a higher dropout. Also, the branching and
35 pruning of the tree branches in BNeuralT are performed at the tree generation stage, where a
36 branch is probabilistically pruned by generating a leaf node at a depth lower than terminals.

¹ **3 Backpropagation neural tree**

² **3.1 Problem statement**

³ Let $\mathcal{X} \in \mathbb{R}^d$ be an instance-space and $\mathcal{Y} = \{c_1, \dots, c_r\}$ be a set of r labels such that a label
⁴ $y \in \mathcal{Y}$ is assigned to an instance $\mathbf{x} \in \mathcal{X}$. Therefore, for a training set of N instance-label pairs
⁵ $\mathcal{S} = (\mathbf{x}_i, y_i)_{i=1}^N$, we induced a classifier $\mathcal{G}(\mathcal{X}, \mathbf{w})$ that reduces classification cost $\mathcal{L}_{\text{Error}}(\mathcal{G}) =$
⁶ $1/N \sum_{i=1}^N (\hat{y}_i \neq y_i)$, where \hat{y}_i is a predicted output class on an input instance $\mathbf{x}_i = \langle x_1^i, x_2^i, \dots, x_d^i \rangle$
⁷ labeled with the target class $y_i \in \{c_1, \dots, c_r\}$. Additionally, when an instance $\mathbf{x} \in \mathcal{X}$ is associated
⁸ with a continuous variable $y \in \mathbb{R}$ rather than a set of discrete class labels, then $\mathcal{G}(\mathcal{X}, \mathbf{w})$ is a
⁹ predictor that for a training set of instance-output pairs \mathcal{S} reduces a prediction cost like mean
¹⁰ squared error (MSE) $\mathcal{L}_{\text{MSE}}(\mathcal{G}) = 1/N \sum_{i=1}^N (\hat{y} - y_i)^2$.

¹¹ **3.2 Backpropagation neural tree algorithm**

¹² Backpropagation neural tree (BNeuralT) takes a tree-like architecture whose root node is a
¹³ decision node, and leaf nodes are inputs. For classification learning problems, BNeuralT has
¹⁴ strictly dedicated nodes at level-1 (child nodes of the root) of the tree to represent classes.
¹⁵ Fig. 1(a) is an example of a *classification neural tree* where root's each immediate child is a sub-
¹⁶ tree dedicated to a class, and the root node only decides a winner class $\hat{y} = \text{argmax}\{c_1, \dots, c_r\}$
¹⁷ for an instance-label pair (\mathbf{x}, y) . For regression learning problems, BNeuralT is a *regression*
¹⁸ *neural tree* whose root node decides the tree's predicted output $\hat{y} = \varphi(\sum_{i=1}^{\text{child}} w_i v_i + b_{v_0})$, where
¹⁹ $\varphi(\cdot)$ is an activation function yielding a value in $[0, 1]$, w_i is a edge weight, v_i is the activation
²⁰ of i -th child, and b_{v_0} is the root's bias (cf. Fig. 1(b)).

²¹ BNeuralT, denoted as \mathcal{G} is an m -ary rooted tree with its one node designated as the root node,
²² and each node takes at least $m \geq 2$ child nodes except for a leaf node that takes no child
²³ node. Hence, for a tree depth p , BNeuralT takes $n \leq [(m^{p+1} - 1)/(m - 1)]$ nodes (including
²⁴ the number of internal nodes $|V|$ and the leaf nodes $|T|$). Thus, BNeuralT can be defined as a
²⁵ union of internal and leaf nodes $\mathcal{G} = V \cup T = \{v_1^j, v_2^j, \dots, v_K^j\} \cup \{t_1, t_2, \dots, t_L\}$ where k -th node
²⁶ $v_k^j \in V$ is an internal node and receives $2 \leq j \leq m$ inputs from its child nodes. The k -th leaf
²⁷ node $t_k \in T$ has no child, and it has a designated input $x_i \in \{x_1, x_2, \dots, x_d\}$.

²⁸ Fig. 1 is an example of classification (left) and regression (right) trees. All internal nodes (shaded
²⁹ in gray) of the tree are neural nodes and may behave like the nodes of a NN. That is, a neural
³⁰ node computes a weighted summation z of inputs and squashes that using an activation function
³¹ $\varphi(z)$, e.g., *sigmoid*: $\varphi(z) = 1/(1 + e^z)$ or *ReLU*: $\varphi(z) = \max(0, z)$. We installed sigmoid or ReLU
³² functions as BNeuralT's neural nodes, which can be any other activation function like *tanh*. The
³³ trainable parameters \mathbf{w} are the edges and the bias weights of the nodes. The number of nodes
³⁴ n in a tree grows as per $\mathcal{O}(m^p)$. The number of edges ($n - 1$) is proportional to the growth of
³⁵ n , so is the number of tree's *trainable parameters* \mathbf{w} .

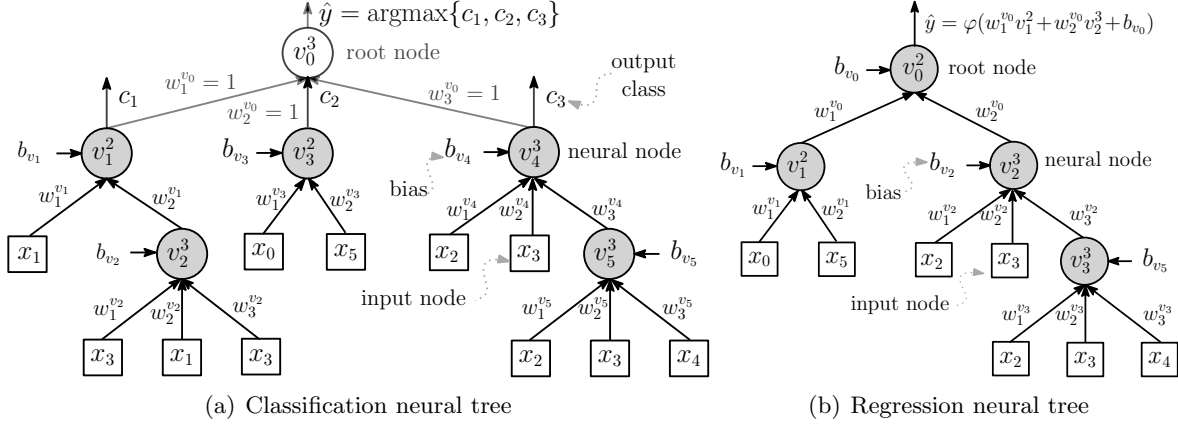


Fig. 1: Neural Trees: (a) A neural tree example of a three-class classification learning problem. The root node v_0^3 takes three immediate children: v_1, v_3 , and v_4 , each respectively designated to a class c_1, c_2 , and c_3 . The internal nodes (shaded in gray) are neural nodes and take an activation function $\varphi(\cdot)$ and leaf nodes are inputs. Each designated output class has its subtree. This tree takes its input from the set $\{x_1, x_2, \dots, x_5\}$. The link $w_i^{v_j}$ between nodes are neural weights. (b) A neural tree example for a regression problem has one output node v_0 .

1 **Complexity of BNeuralT.** A BNeuralT model resembles an expression tree, and its computation
2 is a depth-first-search post-order or pre-order traversal where each node needs to be visited
3 at least once. Hence, the worst-case *time complexity* of BNeuralT is $\mathcal{O}(n)$, n being the number
4 of nodes. In a BNeuralT model, each internal node has a bias, each leaf has an input, and each
5 edge has a weight. Therefore, the space requirement of a BNeuralT model is $2|V| + |T|$, i.e., two
6 times internal nodes plus leaf nodes, which will grow proportional to the growth of tree's total
7 nodes $n = |V| + |T|$. Thus, BNeuralT's worst-case *space complexity* is $\mathcal{O}(n)$.

8 **Biologically plausible neural computation of BNeuralT.** A typical NN uses McCulloch
9 and Pitts (1943) neurons. Such a neuron operates on a weighted sum of inputs and processes the
10 sum via a nonlinear threshold function. Such neural computation considers that the dendrites
11 (synaptic inputs) of a neuron are summed at “soma,” thereby exciting a neuron, i.e., providing
12 it a firing strength (McCulloch and Pitts, 1943; Hodgkin and Huxley, 1952; Poirazi et al.,
13 2003a). However, the biological behavior of dendrites shows that dendrites themselves impose
14 nonlinearity on their synaptic inputs before summing at “soma” (London and Häusser, 2005;
15 Hay et al., 2011). This dendritic nonlinearity is possibly a sigmoidal nonlinearity (Poirazi et al.,
16 2003b). Additionally, the synaptic connections in a fully connected NN are symmetric, whereas
17 biological dendritic connections are asymmetric (Mel, 2016; Travis et al., 2005; Farhoodi and
18 Kording, 2018) [cf. Fig. 2(a)].

19 Poirazi et al. (2003b) using a sparse two-layer NN analogous to a binary tree-like dendritic NN
20 has shown the possibility of modeling a single neuron as a NN. The work of Beniaguev et al.
21 (2020) demonstrated a proof of concept single neuron model as a synaptic *integration and fire*
22 model capable of performing classification of two types of classes with a high degree of temporal

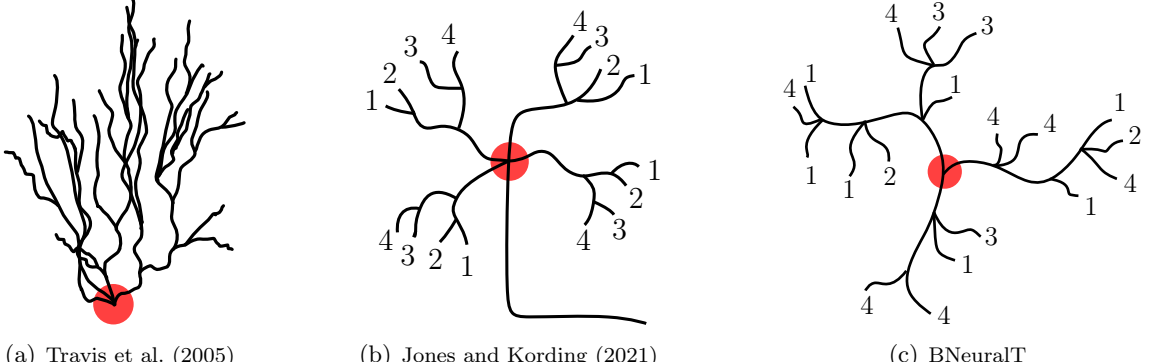


Fig. 2: Biologically plausible neural computation using *dendritic trees*. Red circle represents a neuron (*soma*), black lines are dendrites, and the numbers indicate inputs.

accuracy. Jones and Kording (2021) considered the biologically asymmetric morphology of “*dendritic tree*” and its repeated synaptic inputs to a neuron to show the computational capability of a *single neuron* for solving machine learning problems.

Fig. 2(b) shows Jones and Kording (2021)’s a single neuron computational model with repeated inputs as a binary tree structure. Unlike the work of Poirazi et al. (2003b), BNeuralT has asymmetric *dendritic connections* to a “*single*” neuron (Beniaguev et al., 2020; Jones and Kording, 2021). Jones and Kording (2021)’s dendritic tree has a systematic and regular binary-tree-like structure and solves a binary classification problem. Whereas BNeuralT’s neuron is like the neuron of Travis et al. (2005) (cf. Fig. 2(a)), and it has a stochastic m -ary rooted tree-like structure (cf. Fig. 2(c)). Through BNeuralT, we investigate the ability of a single neuron with sigmoidal nonlinearity (and linear when using ReLU) in its dendritic connections on three machine-learning problems: multi-class classification, regression, and pattern recognition.

Stochastic gradient descent (SGD) training. BNeuralT’s trainable parameters \mathbf{w} are iteratively optimized by a stochastic gradient descent (SGD) method (cf. Algorithm 1) that at an iteration j requires gradient $\nabla \mathbf{w}_j \leftarrow \text{GRADIENT} \nabla_{\mathbf{w}} \mathcal{L}(\mathbf{x}_j, \mathcal{G}_{\mathbf{w}_j})$ computation (cf. Algorithm 2) and weight update as per $\mathbf{w}_j \leftarrow \mathbf{w}_{j-1} + \eta \nabla \mathbf{w}_j$. The weight update $\mathbf{w}_j \leftarrow \mathbf{w}_{j-1} + \eta \nabla \mathbf{w}_j$ in line number 7 of Algorithm 1 is a simple GD method, where other similar optimizers like MGD, NAG, Adagrad, RMSprop, or Adam can also be used. Table 1 details the expressions of weight updates for these optimizers.

Error-backpropagation in BNeuralT. Our proposed *recursive error-backpropagation* in BNeuralT algorithm has two computation phases: *forward pass* and *backward pass* (cf. Fig. 3). Both work in a *depth-first search* manner. Since a tree data structure is algorithmically recursive to traverse through, both forward pass and backward (error-backpropagation) pass take place in a recursive manner. The forward pass computation produces the output for a tree in a *post-order traversal* manner (cf. Fig. 3(left)). That is, each leaf node propagates its input through dendrite

Algorithm 1 Stochastic gradient descent (SGD)

```

1: procedure SGD( $\mathcal{G}_w$ ,  $\mathcal{S}$ )                                 $\triangleright$  takes a neural tree  $\mathcal{G}_w$  and training data  $\mathcal{S}$ 
2:    $w_0 \leftarrow \mathcal{G}_w$                                 $\triangleright$  initial weights
3:   for epoch $_i < \text{epoch}_{\max}$  do
4:      $\mathcal{S} \leftarrow \text{SHUFFLE}(\mathcal{S})$             $\triangleright$  function SHUFFLE returns a randomly shuffle dataset
5:     for an instance  $\mathbf{x}_j \in \mathcal{S}$  do
6:        $\Delta w_j \leftarrow \text{GRADIENT } \nabla_w \mathcal{L}(\mathbf{x}_j, \mathcal{G}_{w_j})$        $\triangleright$  computed as per Algorithm 2
7:        $w_j \leftarrow w_{j-1} + \eta \Delta w_j$            $\triangleright$  GD weights update on an input instance  $\mathbf{x}_j$ 
8:     end for
9:   end for
10:  end procedure

```

Table 1: Gradient descent versions to replace line number 7 in Algorithm 1. Symbols $\eta, \gamma, \beta, \beta_1$, and β_2 are constants (hyperparameter) of respective algorithms. Symbol v_j and w_j show previous momentum and weights, respectively, and $\nabla_w \mathcal{L}(\mathbf{x}_j, \mathcal{G}_{w_j})$ shows gradient of loss \mathcal{L} over input \mathbf{x}_j and w of tree \mathcal{G} .

Algorithm	Expression
MGD (Qian, 1999)	$v_j \leftarrow \gamma v_{j-1} + \eta \nabla_w \mathcal{L}(\mathbf{x}_j, \mathcal{G}_{w_j})$ $w_j \leftarrow w_{j-1} - v_j$
Nesterov accelerated GD (Bengio et al., 2013)	$v_j \leftarrow \gamma v_{j-1} + \eta \nabla_w \mathcal{L}(\mathbf{x}_j, \mathcal{G}_{w_j - w_{j-1}})$ $w_j \leftarrow w_{j-1} - v_j$
Adagrad (Dean et al., 2012)	$v_j \leftarrow v_{j-1} + \nabla_w \mathcal{L}(\mathbf{x}_j, \mathcal{G}_{w_j})^2$ $w_j \leftarrow w_{j-1} - \eta / \sqrt{v_j + \epsilon} \nabla_w \mathcal{L}(\mathbf{x}_j, \mathcal{G}_{w_j})$
RMSprop (Tieleman and Hinton, 2012)	$v_j \leftarrow (1 - \gamma) v_{j-1} + \gamma \nabla_w \mathcal{L}(\mathbf{x}_j, \mathcal{G}_{w_j})^2$ $w_j \leftarrow w_{j-1} - (\eta / \sqrt{v_j + \epsilon}) \nabla_w \mathcal{L}(\mathbf{x}_j, \mathcal{G}_{w_j})$
Adam (Kingma and Ba, 2015)	$m_j \leftarrow \beta_1 m_{j-1} + (1 - \beta_1) \nabla_w \mathcal{L}(\mathbf{x}_j, \mathcal{G}_{w_j}) / (1 - \beta_1^j)$ $v_j \leftarrow \beta_2 v_{j-1} + (1 - \beta_2) \nabla_w \mathcal{L}(\mathbf{x}_j, \mathcal{G}_{w_j})^2 / (1 - \beta_2^j)$ $w_j \leftarrow w_{j-1} - \eta / (\sqrt{v_j + \epsilon}) m_j$

- ¹ (edge) to its parent node, and subsequently, each internal node, after computing received inputs
² from its child nodes, propagates activation to their respective parent node. Finally, the root
³ node computes the tree’s output.
- ⁴ The backward pass computes the gradient of the error with respect to edge weights. The
⁵ backward pass computes gradient δ for each internal node and propagates it back to each edge
⁶ depth-by-depth. Hence, the backward pass is a *pre-order traversal* of the tree (cf. Fig. 3(right)).
⁷ That is gradient δ computed at the root node flow backward to its child node until it reaches
⁸ leaf nodes. Fig. 4 (left) shows the forward pass and backward pass computation labeled with
⁹ variables of neural tree computation. Fig. 4 (right) shows the backpropagation of gradient from
¹⁰ an output node to the inputs (leaf nodes). Algorithm 2 is a summary of error-backpropagation
¹¹ and Algorithm 3 shows recursive gradient computation for BNeuralT that facilitates error-
¹² backpropagation.

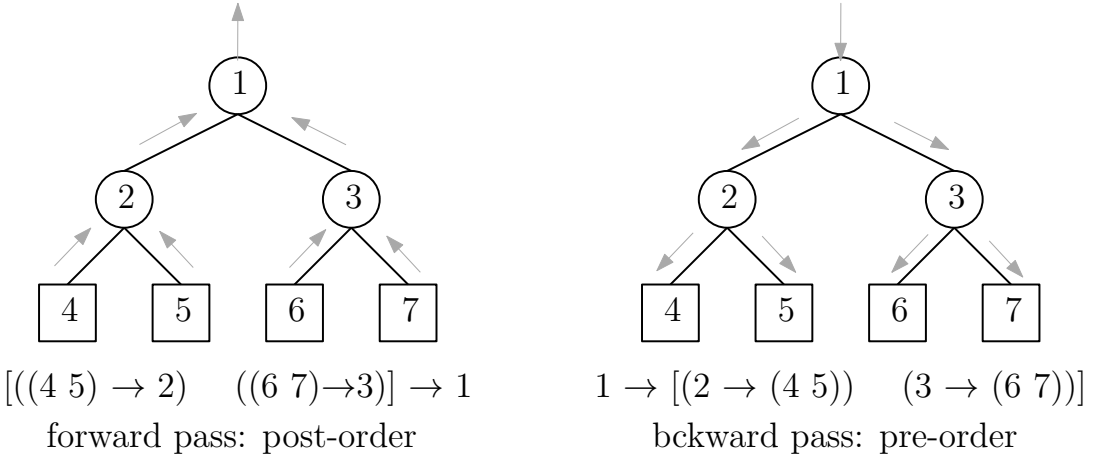


Fig. 3: Forward pass (left) and backward pass (right) computation. The arrows show the direction of computation.

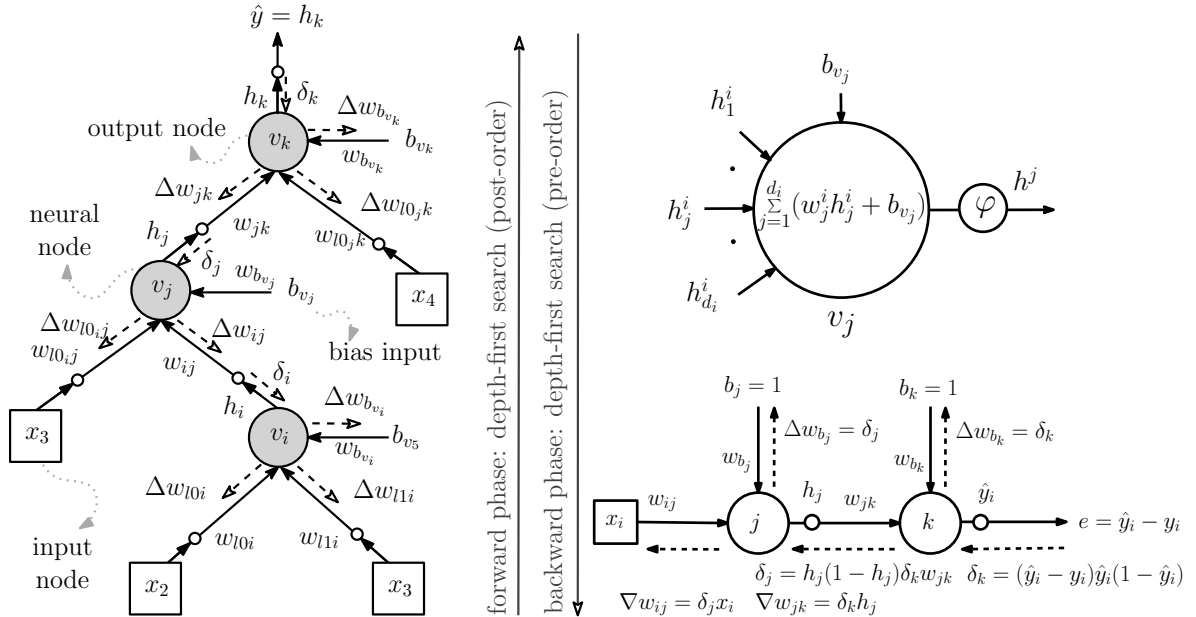


Fig. 4: *Left.* Backpropagation Neural Tree. Output node v_k yields output y using forward pass upon receiving inputs x_i from leaf nodes. Each node is linked with an edge weight w_{ij} . The backward pass propagates error $e = (y - \hat{y})$ back to input nodes to compute weight change Δw . *Right.* Backpropagation of error from an output node, k ; to a hidden node, j ; to an input node, i ; and to bias inputs b_k and b_j . Dashed lines represent error backpropagation and computation δ and gradient ∇w (cf. Algorithm 2) to find weight change Δw that help stochastic gradient descent (cf. Algorithm 1).

Algorithm 2 Backpropagation computation of neural tree \mathcal{G}

```
1: procedure GRADIENT  $\nabla \mathbf{w} \mathcal{L}(\mathbf{x}, \mathcal{G})$        $\triangleright \mathbf{x}$  and  $\mathbf{w}$  are the inputs and trainable parameters
2:    $\mathcal{G}_\delta \leftarrow \text{COMPUTE } \delta(y, \mathcal{G}(\mathbf{x}), N_0 \leftarrow \mathcal{G}, \mathcal{G})$      $\triangleright$  Compute  $\delta$  using Algorithm 3 for target  $y$ 
   and prediction  $\mathcal{G}(\mathbf{x})$  at tree's root  $N_0$ 
3:   for all nodes  $N$  in  $\mathcal{G}_\delta$  do
4:     if  $N \rightarrow Type \rightarrow$  Output node then            $\triangleright$  output node's bias weight update
5:        $N \rightarrow \nabla w_{b_k} = N \rightarrow \delta_k$            $\triangleright$  bias weight is set to current node's gradient  $\delta$ 
6:     else if  $N \rightarrow Type \rightarrow$  Internal (hidden) node then
7:        $h_j = N \rightarrow h_j$            $\triangleright$  current node's activation is the incoming signal for weight  $w_{jk}$ 
8:        $\delta_k = N \rightarrow N_{Parent} \rightarrow \delta$          $\triangleright$  gradient back-propagated from the parent node
9:        $N \rightarrow \nabla w_{jk} = \delta_k h_j$      $\triangleright w_{jk}$  is the weight between node  $N_j$  and its parent node  $N_k$ 
10:       $N \rightarrow \nabla w_{b_j} = N \rightarrow \delta_j$          $\triangleright$  bias weight is set to current node's gradient  $\delta$ 
11:     else if  $N \rightarrow Type \rightarrow$  Leaf node then
12:        $x_i = N \rightarrow x$            $\triangleright N \rightarrow x \in \{x_1, x_2, \dots, x_d\}$  is an input attribute
13:        $\delta_j = N \rightarrow N_{Parent} \rightarrow \delta$          $\triangleright$  gradient back-propagated from parent to child
14:        $N \rightarrow \nabla w_{ij} = \delta_j x_i$          $\triangleright w_{ij}$  is the weight between child  $N_i$  and parent  $N_j$ 
15:     end if
16:   end for
17: return  $\nabla \mathbf{w}$ 
18: end procedure
```

Algorithm 3 Computation of δ for each neural node

```
1: procedure COMPUTE  $\delta(y, \hat{y}, N \leftarrow \mathcal{G}, \mathcal{G})$      $\triangleright y$  is a target,  $\hat{y}$  is a prediction, and  $N$  is the
   current (or entry) node of tree  $\mathcal{G}$ 
2:   if  $N \rightarrow Type \rightarrow$  Output node then       $\triangleright$  compute gradient  $\delta_k$  for output node  $N$  in  $\mathcal{G}$ 
3:      $N \rightarrow \delta_k = (\hat{y} - y)\hat{y}(1 - \hat{y})$            $\triangleright$  gradient at sigmoid output node
4:   else                                      $\triangleright$  compute gradient at an internal (hidden) neural node
5:      $h_j = N \rightarrow h_j$            $\triangleright$  activation (value) of an internal (neural) node
6:      $\delta_k = N \rightarrow N_{Parent} \rightarrow \delta_k$          $\triangleright$  retrieve parent's gradient  $\delta$  of the current node  $N$ 
7:      $w_{jk} = N \rightarrow w_{jk}$            $\triangleright$  edge (weight) between current node  $N_j$  and parent node  $N_k$ 
8:      $N \rightarrow \delta_j = h_j(1 - h_j)\delta_k w_{jk}$          $\triangleright$  gradient at an internal sigmoid node
9:   end if
10:  for all child (neural) node  $N_c$  of  $N$  in  $\mathcal{G}$  do
11:     $\mathcal{G}_\delta \leftarrow \text{COMPUTE } \delta(\emptyset, \emptyset, N_c \leftarrow \mathcal{G}, \mathcal{G})$   $\triangleright$  call COMPUTE  $\delta$ ,  $\emptyset$  indicates unused argument
12:  end for
13: end procedure
```

4 Experiments

4.1 Hyperparameters settings

Datasets: We select a set of nine *classification problems*: Australia (Aus), Heart (Hrt), Ionosphere (Ion), Pima (Pma), Wisconsin (Wis), Iris (Irs), Wine (Win), Vehicle (Vhl), Glass (Gls), which respectively have 14, 13, 33, 8, 30, 4, 13, 18, and 9 input attributes; 2, 2, 2, 2, 2, 3, 3, 4, and 7 target classes; and 690, 270, 351, 768, 569, 150, 178, 846, and 214 examples. For

1 *regression problems*, we select Baseball (Bas), Daily Electricity Energy (Dee), Diabetes (Dia),
2 Friedman (Frd), and Miles Per Gallon (Mpg), which respectively have 16, 6, 10, 5, and 6 input
3 attributes and 337, 365, 442, 1200, and 392 examples. Each regression dataset has one target.
4 These datasets are available at (Bache and Lichman, 2013; Keel, 2011). These problems are
5 significantly different not only in terms of the number of classes and examples but also in terms
6 of their attribute types and range. This differing nature of these problems poses significant
7 variations in difficulty for one algorithm to excel on all problems (Wolpert, 1996).

8 Both classification and regression learning datasets were *normalized* using min-max normalization
9 between 0 and 1. Each dataset was randomly shuffled and partitioned into training (80%)
10 and test (20%) sets for each instance of the experiment. For a *pattern recognition* problem, we
11 select the MNIST dataset (LeCun et al., 2020), which has 60,000 training examples and 10,000
12 test examples labeled with a set of 10 handwritten characters, and this dataset was normalized
13 by dividing gray-scale pixel value by 255.

14 **BNeuralT hyperparameters.** We repeated experiments 30 times (independently) for each
15 classification and regression problem. In each run, we generated ad hoc BNeuralTs (stochasti-
16 cally generated tree structures) for each dataset with a maximum tree depth $p = 5$; max child
17 per node $m = 5$, and branch pruning factor $P[\text{leaf}_p < p] \in \{0.4, 0.5\}$ which is a probability of a
18 leaf node being generated at a depth lower than the tree height p . A higher leaf generation prob-
19 ability (e.g., 0.5) at internal nodes means that tree height terminates earlier than its predefined
20 depth, which means a tree will be generated with fewer parameters. A lower leaf generation
21 probability (e.g., 0.4) means a deeper tree structure with more parameters.

22 For classification problems, BNeuralT’s output neural node was *argmax* node (i.e., winner takes
23 all node), whereas, for regression problems, it was *sigmoid* activation function. Its internal nodes
24 were *sigmoid* activation (or *ReLU* for some trial experiment versions). For pattern recognition
25 (MNIST dataset), BNeuralT models were generated on an ad hoc basis via setting maximum
26 tree depth $p \in \{5, 10\}$, and max child per node $m \in \{10, 15\}$ with $P[\text{leaf}_p < p] \in \{0.4, 0.5\}$ and
27 a tree size threshold $|\mathcal{G}|_{\geq \text{MIN}} \in \{1K, 20K\}$, where “K” is 1000.

28 **Other algorithms hyperparameters.** MLP architecture was a fixed three-layer architecture
29 [inputs–hidden (100 nodes)–targets] for each dataset of classification and regression problems.
30 A *SoftMax* layer acted as the MLP classifier’s output nodes, and an MLP regression had a
31 *sigmoid* activation as its output node. The internal neural nodes in an MLP were *sigmoid* (or
32 *ReLU*) functions. Other algorithms HFNT^S, HFNT^M, MONT₃, DT, RF, GP, NBC, SVM, and
33 CARTs had their default setups as they are in their libraries (Pedregosa et al., 2011) or in the
34 literature (Ojha et al., 2017; Ojha and Nicosia, 2020; Zharmagambetov et al., 2019). A detailed
35 list of hyperparameters of all algorithms is provided in Supplementary Table A1.

36 **SGD hyperparameters.** BNeuralT and MLP algorithms take *optimizers* like GD, MGD,

1 NAG, Adagrad, RMSprop, or Adam. The training parameters were learning rate $\eta = 0.1$,
 2 momentum rate $\gamma = 0.9$, $\beta_1 = 0.9$, $\beta_2 = 0.9$, $\epsilon = 1e^{-8}$, training mode was *stochastic* (online), and
 3 training epochs were 500. Since the gradient descent computation was stochastic, both BNeuralT
 4 and MLP do the same number of forward-pass (function) evaluations, i.e., number training
 5 examples \times epochs. All six optimizers were used for training BNeuralT and MLP with an *early-*
 6 *stopping* restore-best strategy (or without an *early-stopping* for some trial experiments), whereas
 7 other algorithms take their own default optimizer (Pedregosa et al., 2011). While BNeuralT and
 8 MLP were trained in *online* mode (example-by-example training), other algorithms take only
 9 *offline* mode (epoch-by-epoch) training.
 10 For the pattern recognition problem (MNIST), we set a *mini-batch* training with a batch size
 11 of 128 examples. RMSprop was used as an *optimizer*, and BNeuralT was trained by varying
 12 learning rate $\eta \in \{0.1, 0.01\}$ and the number of epochs $\in \{10, 25, 50, 70\}$. The results of other
 13 algorithms on MNIST were collected from literature to compare performances.
 14 **Loss functions.** The loss function for BNeuralT training for classification and pattern recogni-
 15 tion problems was a miss-classification rate $\mathcal{L}_{\text{Error}}(\mathcal{G})$. MLP training on classification problems
 16 was best with categorical cross-entropy loss (Bishop, 2006). The training of other algorithms had
 17 default setups recommended in their libraries (Pedregosa et al., 2011). For regression problems,
 18 all algorithms were trained by reducing $\mathcal{L}_{\text{MSE}}(\cdot)$. The test metric for classification problems
 19 for all algorithms was a miss-classification rate $\mathcal{L}_{\text{Error}}(\cdot)$ and for regression problems, it was a
 20 regression fit $\mathcal{L}_{r^2}(\cdot) = 1 - \sum_{i=1}^N (y_i - \hat{y}_i)^2 / \sum_{i=1}^N (y_i - \bar{y})^2$ (Nash–Sutcliffe model efficiency coefficient)
 21 which gives a value between $[-\infty, 1]$, where \bar{y} is the mean of target y .
 22 **Forward pass computation time, τ .** BNeuralT was implemented in Java 11, and MLP
 23 was implemented using TensorFlow and Keras libraries (Keras, 2020). Other algorithms were
 24 implemented using scikit-learn library (Pedregosa et al., 2011) in Python 3.5. The forward pass
 25 computation time, τ is a wall-clock time on Windows 10 operating system with configuration
 26 x64 Intel i5-2400 CPU, 3.1GHz, 3101Mhz, 4 Cores, and 16GB physical memory.

27 4.2 BNeuralT and MLP experiment versions

28 We experimented with multiple versions of BNeuralT and MLP settings to bring out the best
 29 of both. We tried *sigmoid* and *ReLU* as the internal activation functions. We tried BNeuralT’s
 30 branch pruning factor $P[\text{leaf}_p < p]$ with 0.5 and 0.4.
 31 The learning rates of the optimizers had two sets: (i) A flat learning rate $\eta = 0.1$ for all
 32 optimizers. (ii) The learning rate recommended in the Keras library for respective optimizers,
 33 i.e., RMSprop, Adam, and Adagrad had $\eta = 0.001$, and MGD, NAG, and GD had $\eta = 0.01$. We
 34 call the library’s recommended η value a *default* learning rate. In addition, the SGD learning
 35 was tried “with” and “without” *early-stopping* (ES) strategies.

These variations produced five BNeuralT settings: (i) ES training of BNeuralT having *sigmoid* nodes, 0.1 learning rate, and 0.5 leaf generation rate; (ii) ES training of BNeuralT having *sigmoid* nodes, *default* learning rate, and 0.5 leaf generation rate; (iii) ES training of BNeuralT having *ReLU* nodes, 0.1 learning rate, and 0.5 leaf generation rate; (iv) ES training of BNeuralT having *sigmoid* nodes, 0.1 learning rate, and 0.4 leaf generation rate; and (v) without ES training of BNeuralT having *sigmoid* nodes, 0.1 learning rate, and 0.5 leaf generation rate.

Multiple MLP settings were tried. Out of which, some best performing settings were: (i) ES training of MLP having *sigmoid* nodes and 0.1 learning rate; (ii) ES training of MLP having *sigmoid* nodes and *default* learning rate; (iii) ES training of MLP having *sigmoid* nodes, 0.1 learning rate, and L2-norm regularization; (iv) ES training of MLP having *sigmoid* nodes, *default* learning rate, and L2-norm regularization; and (v) experiment setting same as (i) but without ES; and (vi) experiment setting same as (ii) but without ES. Other trials were using dropout with and without early stopping.

For each algorithm (BNeuralT, MLP, HFNT^S, HFNT^M, MONT₃, DT, RF GP, NBC, and SVM), each optimizer (GD, MGD, NAG, Adagrad, RMSprop, and Adam), and each variation of hyperparameter setting, there were 110 experiments (cf. Tables A2 and A3 in Supplementary). We repeated each experiment for each dataset for 30 independent runs, and their average performance on test sets was evaluated.

5 BNeuralT performance

5.1 Selection of the best performing setting

We selected the best performing setting based on the average test accuracy computed over 30 independent runs of BNeuralT, MLP, HFNT^S, HFNT^M, MONT₃, DT, RF, GP, NBC, and SVM to report them in detail in this section. The best performing BNeuralT setting was the “ES training of BNeuralT having *sigmoid* nodes, 0.1 learning rate, and 0.4 leaf generation rate.” The best MLP setting was “ES training of MLP having *sigmoid* nodes and *default* learning rate.” We found that HFNT^S, HFNT^M, DT, RF, GP, NBC, and SVM worked best with their recommended setting.

We found that collectively on all classification and regression datasets, BNeuralT with *sigmoid* nodes, 0.1 learning rate, and 0.4 leaf generation rate trained using RMSprop performed the best among all experiment versions of all algorithms. This setting produced an average accuracy of 83.2% across all datasets with an average of 222 trainable parameters. This same setting also performed the best across all classification datasets among all algorithms, i.e., it produced an average accuracy of 89.1% with an average of 261 trainable parameters. In fact, the top six best results over classification datasets were from BNeuralT settings. GP algorithm came 7th with an average classification accuracy of 86.79%. MLP with *sigmoid* node and ES training using

1 MGD optimizer with *default* learning performed 8th with an average accuracy of 86.78% with
2 an average 1970 trainable parameters.

3 MLP, however, performed slightly better on regression problems than the other algorithms. MLP
4 with *sigmoid* node and ES training using NAG optimizer with *default* learning rate produced an
5 average regression fit value of 0.775. Whereas BNeuralT with *sigmoid* nodes, 0.1 learning rate,
6 and 0.4 leaf generation rate trained using RMSprop optimizer produced an average regression
7 fit value of 0.727. It is important to note that this performance of BNeuralT comes with a much
8 lower average trainable parameter. BNeuralT used only 152 trainable parameters compared to
9 MLP that used 1041 parameters. This means BNeuralT’s performance comes with an order
10 magnitude less parameter than MLP on both classification and regression tasks.

11 Table 2 reports the details of each algorithm’s best-performing settings. However, exhaustive
12 lists of 110 experiments, from which we selected these best performing settings, are provided in
13 Supplementary Tables A2 and A3.

14 5.2 BNeuralT models summary

15 **BNeuralT classification models summary.** Table 2 suggests that BNeuralT performance
16 on both classification and regression problems is highly competitive with MLP and other al-
17 gorithms. For example, the average performance of BNeuralT’s RMSprop on all classification
18 problems is 2.65% (average accuracy: 89.1%) higher than the nearest best performing non-
19 BNeuralT algorithm. The best MLP model offered an average accuracy of 86.8%, and MLP
20 with a 0.4 dropout rate using Adam produced an 85.9% accuracy. Other algorithms were as
21 follows: HFNT^S, 78.9%; HFNT^M, 72.4%; MONT₃, 83.1%; DT, 81.3%; RF, 86.4%; GP, 86.8%;
22 NBC, 78.2%; and SVM, 84.1%. For this performance, BNeuralT uses *only* 13.25% ($w = 261$)
23 trainable parameters than MLP’s 1969 parameters. The structures of some select best perform-
24 ing BNeuralT classification models are shown in Fig. 5, where black edges indicate dendrites;
25 and green, blue, red, and black nodes, respectively indicate inputs, dendritic nonlinearities, root,
26 and class nodes.

27 The average tree size of BNeuralT with $P[\text{leaf}_p < p] = 0.5$ and RMSprop was 119 (89% accuracy).
28 The average tree size of HFNT^M, MONT₃, and HFNT^S algorithms were 29 (72.4% accuracy),
29 36 (83.1% accuracy), and 92 (78.9% accuracy), respectively. Since tree construction and forward
30 pass computation are similar for BNeuralT, HFNT, and MONT algorithms, there is a trade-off
31 between the model’s compactness and accuracy. In fact, this produces a set of trade-off solutions
32 (between accuracy and complexity). Along with this set of Pareto solutions, one can choose
33 which is the best candidate solution for the given machine learning problem under examination:
34 more accurate but less sustainable or a little less accurate but more robust and sustainable.

35 The forward pass computation time on a single example (in multiple of 10^{-6} seconds) of BNeu-

1 ralT was 11.2 seconds, whereas MLP took 1288; DT, 3.1; RF, 485.4; GP, 455.6; NBC, 31.9; and
2 SVM, 16.1 seconds. DT was the fastest, and BNeuralT was the second-fastest. However, DT
3 has a much lower accuracy (81.3%) than BNeuralT (89.1%). The time computation is difficult
4 to compare as the algorithms were implemented in different programming languages (Pereira
5 et al., 2017). BNeuralT was implemented in Java 11, and all other algorithms were implemented
6 in Python 3.5. However, BNeuralT’s performance on classification problems was clearly better
7 among all algorithms. This is further evident from BNeuralT’s collective average accuracy of all
8 optimizers on all classification datasets was 86.1%. Whereas on all optimizers, MLP’s average
9 accuracy was 83.8%, trees algorithms had 80.4%, and other algorithms had 83.6% accuracy.

10 We selected BNeuralT’s best optimizer RMSprop for the statistical significance test. This test
11 was designed to examine whether the performance of BNeuralT’s RMSprop is statistically sig-
12 nificant than that of the other algorithms. Table 3 presents Kolmogorov–Smirnov (KS) test
13 results on two samples to examine the *null hypothesis* that there is no difference between the
14 performance distributions of BNeuralT’s RMSprop and other algorithms. The results show that
15 for most datasets and most algorithms, the classification results of BNeuralT’s RMSprop show
16 statistical significance over other algorithms’ performance as the *null hypothesis* of no difference
17 is rejected in most cases. This was the case, despite using a restrictive Bonferroni correction to
18 adjust p-values. Wilcoxon signed-rank test and Independent T-test in Supplementary Table A4
19 and Table A5 also favor BNeuralT’s RMSprop.

20 **BNeuralT regression models summary.** MLP’s Adam performed best for regression prob-
21 lems. MLP’s Adam produced an average regression fit of 0.772 without dropout and 0.754 with
22 dropout on all datasets. BNeuralT’s RMSprop offered an average regression fit of 0.727, which
23 differs only by 5.8% with the best MLP result. This performance of BNeuralT comes with the
24 use of only 14.6% trainable parameters than the parameters used by the MLP ($w = 1014$). (Note
25 that an MLP dropout model during its test phase uses all weights since dropout only regularizes
26 weights by averaging gradient over epochs during the training phase (Srivastava et al., 2014).)
27 This suggests that BNeuralT is highly capable of learning data with very low complexity with a
28 faster forward pass computation time. The structure of some select best performing BNeuralT
29 regression models is shown in Fig. 6.

30 The average tree size of BNeuralT with $P[\text{leaf}_p < p] = 0.5$ and RMSprop for regression problems
31 was 64 ($\mathcal{L}_{r2} = 0.675$). The average tree size of HFNT^S and HFNT^M algorithms were 127
32 ($\mathcal{L}_{r2} = 0.562$) and 90 ($\mathcal{L}_{r2} = 0.567$) respectively. Here, BNeuralT was able to perform accurately
33 compared to genetically optimized HFNT algorithms with less complex models.

34 The statistical tests in Table 3 also suggest that BNeuralT’s RMSprop performance distribution
35 on regression problems compared with MLP’s Adam is statistically insignificant *only* on the
36 Friedman dataset. On all other regression datasets, BNeuralT’s RMSprop performance is equally
37 significant as other algorithms.

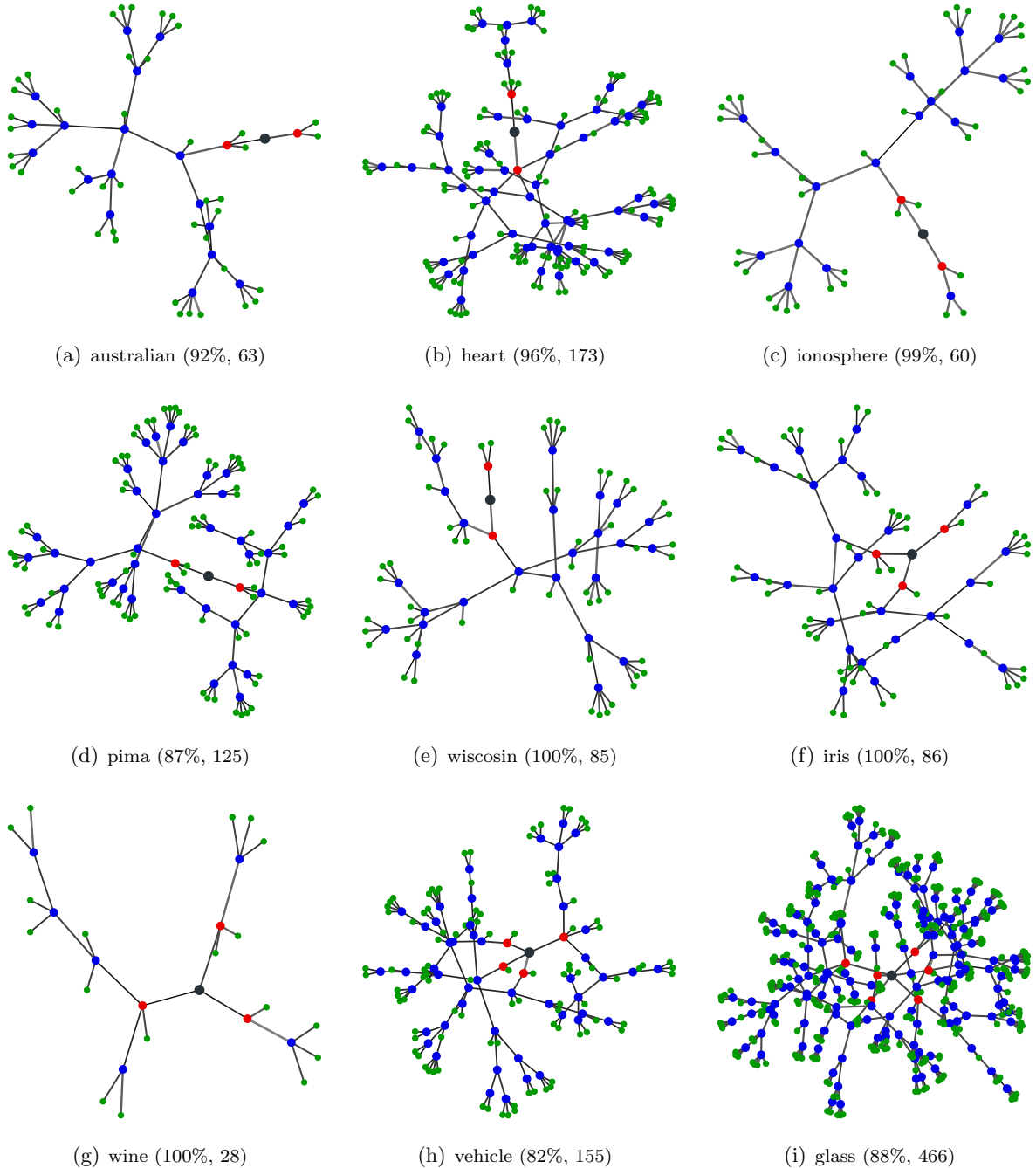


Fig. 5: Classification Trees. (a) - (i) show test accuracy and tree size of select high performing trees of datasets. The black node in a tree is its root node, class output nodes are in red, function nodes are in blue, and leaf nodes are green. The link connecting nodes are neural weights.

Table 2: BNeuralT and other algorithms performance as per average (avg.) accuracy ($1 - \mathcal{L}_{\text{Error}}(\cdot)$) and avg. regression fit ($\mathcal{L}_{r^2}(\cdot)$) on the test sets of 30 independent runs for nine classification and five regression learning problems. Both accuracy and regression fit take 1.0 as the best value. Trainable parameters (\mathbf{w}) of BNeuralT and MLP are neural weights. The best accuracy among all algorithms is marked in bold. Both BNeuralT and MLP are trained on an online mode, whereas other algorithms take offline mode training. Average forward pass (single example prediction time) wall-clock time is $\tau \times 10^{-6}$ seconds (a lower value is better), where τ^J and τ^P respectively indicate time for Java 11 and Python 3.7. Symbol $\mathcal{M}_{0.4}$ indicates MLP with a dropout rate of 0.4, (Avg.) indicates the average performance of an optimizer over datasets, and [Avg.] indicates the average performance of optimizers on a dataset. The classifier results of models MONT₃ and HFNT^M are from Ojha and Nicosia (2020). RF[†] indicates random forest which is an ensemble model.

Algorithm	Avg. classification accuracy [$1 - \mathcal{L}_{\text{Error}}(\cdot)$]										Avg. regression fit $\mathcal{L}_{r^2}(\cdot)$						
	Aus	Hrt	Ion	Pma	Wis	Irs	Win	Vhl	Gls (Avg.)	Bas	Dee	Dia	Frd	Mpg (Avg.)			
BNeuralT (\mathcal{G})	GD	.862	.848	.874	.789	.968	.947	.953	.671	.580	.832	.485	.748	.323	.653	.803	.602
	MGD	.886	.879	.935	.806	.980	.988	.980	.726	.687	.874	.585	.804	.434	.763	.849	.687
	NAG	.886	.878	.938	.808	.980	.987	.978	.731	.688	.875	.585	.804	.434	.757	.851	.686
	Adagrad	.872	.852	.907	.780	.974	.966	.981	.697	.638	.852	.621	.819	.432	.820	.851	.708
	RMSprop	.895	.897	.952	.822	.986	.992	.991	.750	.732	.891	.665	.837	.492	.776	.867	.727
	Adam	.875	.866	.870	.791	.982	.978	.974	.599	.657	.843	.579	.765	.360	.587	.825	.623
	[Avg.]	.880	.870	.913	.799	.978	.976	.976	.696	.663	.861	.587	.796	.412	.726	.841	.672
MLP (\mathcal{M})	GD	.870	.831	.880	.763	.979	.968	.973	.806	.614	.854	.697	.821	.481	.736	.844	.716
	MGD	.874	.831	.907	.774	.981	.977	.985	.853	.629	.868	.718	.826	.486	.804	.852	.737
	NAG	.873	.828	.902	.772	.980	.976	.984	.852	.640	.868	.718	.826	.485	.786	.851	.733
	Adagrad	.870	.827	.723	.670	.944	.736	.877	.462	.362	.719	.407	.584	.221	.571	.630	.482
	RMSprop	.874	.832	.872	.758	.980	.969	.991	.804	.605	.854	.718	.826	.486	.866	.866	.752
	Adam	.876	.833	.882	.774	.984	.972	.991	.826	.635	.863	.721	.829	.490	.943	.874	.772
	[Avg.]	.873	.830	.861	.752	.975	.933	.967	.767	.581	.838	.663	.785	.442	.784	.820	.699
Trees	$\mathcal{M}_{0.4}$ Adam	.871	.815	.912	.774	.971	.960	.973	.806	.645	.859	.707	.828	.491	.884	.862	.754
	HFNT ^S	.824	.825	.871	.754	.973	.912	.918	.481	.544	.789	.576	.794	-0.062	.728	.775	.562
	HFNT ^M	.826	.77	.822	.716	.935	.811	.824	.409	.399	.724	.608	.803	-0.13	.715	.838	.567
	MONT ₃	.889	.809	.898	.799	.962	.989	.952	.55	.629	.831						
	DT	.801	.744	.890	.705	.932	.943	.897	.708	.698	.813	.431	.656	-0.12	.689	.756	.484
	RF [†]	.868	.809	.930	.752	.962	.959	.981	.745	.768	.864	.663	.829	.442	.871	.871	.735
	[Avg.]	.842	.791	.882	.745	.953	.923	.914	.579	.608	.804	.458	.605	.081	.601	.633	.476
Others	GP	.861	.820	.916	.769	.970	.960	.983	.843	.689	.868	.648	.820	.484	.724	.801	.695
	NBC	.797	.833	.882	.758	.930	.953	.969	.455	.457	.782						
	SVM	.861	.841	.880	.769	.977	.926	.978	.762	.575	.841	.647	.838	.405	.912	.861	.733
	[Avg.]	.840	.831	.893	.765	.959	.946	.977	.687	.574	.830	.648	.829	.445	.818	.831	.714
Parameter and Time	\mathbf{w}_G	204	560	185	157	268	180	358	249	190	261	140	163	140	141	178	152
	$\mathbf{w}_M \mathbf{w}_{M_{0.4}}$	1702	1606	1602	3602	803	1102	2304	1703	3302	1969	1801	801	1201	701	701	1041
	τ_G^J	8.5	8.5	6.7	9.6	7.2	15.4	9.3	11.3	24.2	11.2	5.1	5.4	5.2	4.7	6.5	5.4
	τ_M^P	1173	802	628	860	410	1452	1206	412	4648	1288	1931	2031	1409	163	1074	1322
	τ_{DT}^P	1.0	4.2	1.9	1.1	1.5	6.4	5.6	1.2	4.5	3.1	2.0	2.6	1.8	0.6	2.0	1.8
	τ_{RF}^P	278.8	547.8	425.6	253.5	277.5	890.6	743.5	257.1	694.1	485.4	195.5	178.0	155.7	91.7	175.0	159.2
	τ_{GP}^P	187.2	58.6	108.7	195.8	197.6	226.1	253.7	2180	692.1	455.6	12.3	13.2	21.7	73.8	18.8	28.0
	τ_{NBC}^P	8.7	42.6	21.1	6.7	9.9	38.9	75.9	11.2	72.1	31.9						
	τ_{SVM}^P	5.8	20.4	15.5	4.5	5.0	36.7	25.9	5.3	25.6	16.1	17.6	15.5	30.7	9.2	12.2	17.1

Table 3: Kolmogorov–Smirnov (KS) test on two samples: BNeuralT’s RMSprop against all other algorithms for each data. The stat, pval, and post respectively indicate KS statistic, two-tailed p -value, and Bonferroni correction post-hoc adjusted p -value. The values are marked in bold where the *null hypothesis* that BNeuralT’s RMSprop and other algorithms come from the same distribution is rejected as per Bonferroni correction.

BNeuralT’s RMSprop vs.		Classification									Regression					
		Aus	Hrt	Ion	Pma	Wis	Irs	Win	Vhl	Gls	Bas	Dee	Dia	Frd	Mpg	
MLP	GD	stat	.43	.63	.73	.70	.47	.67	.60	.63	.70	.27	.30	.23	.73	.43
		pval	.01	0	0	0	0	0	0	0	0	.24	.14	.39	0	.01
		post	.07	0	0	0	.03	0	0	0	0	1	1	1	0	.06
	MGD	stat	.40	.63	.53	.60	.43	.47	.30	.87	.60	.30	.20	.20	.20	.37
		pval	.02	0	0	0	.01	0	.14	0	0	.14	.59	.59	.59	.03
		post	.16	0	0	0	.07	.03	1	0	0	1	1	1	1	.31
	NAG	stat	.43	.63	.63	.57	.43	.47	.33	.87	.53	.30	.20	.17	.33	.33
		pval	.01	0	0	0	.01	0	.07	0	0	.14	.59	.81	.07	.07
		post	.07	0	0	0	.07	.03	.71	0	0	1	1	1	.64	.64
MLP	Adagrad	stat	.43	.67	1	1	.87	1	.83	1	1	.83	1	.93	.93	1
		pval	.01	0	0	0	0	0	0	0	0	0	0	0	0	0
		post	.07	0	0	0	0	0	0	0	0	0	0	0	0	0
	RMSprop	stat	.33	.60	.77	.67	.40	.50	.23	.60	.73	.30	.23	.20	.57	.20
		pval	.07	0	0	0	.02	0	.39	0	0	.14	.39	.59	0	.59
		post	.71	0	0	0	.16	.01	1	0	0	1	1	1	0	1
	Adam	stat	.30	.63	.67	.63	.47	.50	.17	.70	.63	.30	.17	.17	1	.20
		pval	.14	0	0	0	0	0	.81	0	0	.14	.81	.81	0	.59
		post	1	0	0	0	.03	.01	1	0	0	1	1	1	0	1
MLP	$\mathcal{M}_{0.4}$ Adam	stat	.37	.50	.53	.57	.40	.77	.30	.63	.70	.30	.40	.17	.50	.17
		pval	.03	0	0	0	.02	0	.14	0	0	.14	.02	.81	0	.81
		post	.45	.01	0	0	.20	0	1	0	0	1	.19	1	.01	1
Trees	HFNT ^S	stat	.67	.70	.87	.70	.53	.53	.73	.93	.73	.47	.37		.40	.40
		pval	0	0	0	0	0	0	0	0	0	0	.03		.02	.02
		post	0	0	0	0	0	0	0	0	0	0	0	0	0	0
	HFNT ^M	stat	.67	.87	.83	.87	.63	.53	.77	1	.87	.43	.40		.63	.43
		pval	0	0	0	0	0	0	0	0	0	.01	.02		0	.01
		post	0	0	0	0	0	0	0	0	0	1	1	1	.85	.85
	DT	stat	.90	.87	.70	.93	.87	.67	.90	.53	.33	.67	.90	.93	.77	.87
		pval	0	0	0	0	0	0	0	0	.07	0	0	0	0	0
		post	0	0	0	0	0	0	0	0	.71	0	0	0	0	0
Trees	RF	stat	.43	.73	.40	.90	.80	.57	.47	.30	.33	.30	.20	.37	.77	.20
		pval	.01	0	.02	0	0	0	0	.14	.07	.14	.59	.03	0	.59
		post	.09	0	.20	0	0	0	.03	1	.92	1	1	.41	0	1
Other	GP	stat	.43	.63	.57	.67	.43	.50	.33	.83	.30	.40	.37	.17	.73	.90
		pval	.01	0	0	0	.01	0	.07	0	.14	.02	.03	.81	0	0
		post	.07	0	0	0	.07	.01	.71	0	1	.14	.31	1	0	0
	NBC	stat	.93	.57	.77	.77	.93	.57	.50	1	.97					
		pval	0	0	0	0	0	0	0	0	0					
		post	0	0	0	0	0	0	.01	0	0					
	SVM	stat	.50	.53	.70	.67	.30	.70	.47	.20	.77	.37	.13	.50	.90	.20
		pval	0	0	0	0	.14	0	0	.59	0	.03	.96	0	0	.59
		post	.01	0	0	0	1	0	.03	1	0	.31	1	.01	0	1

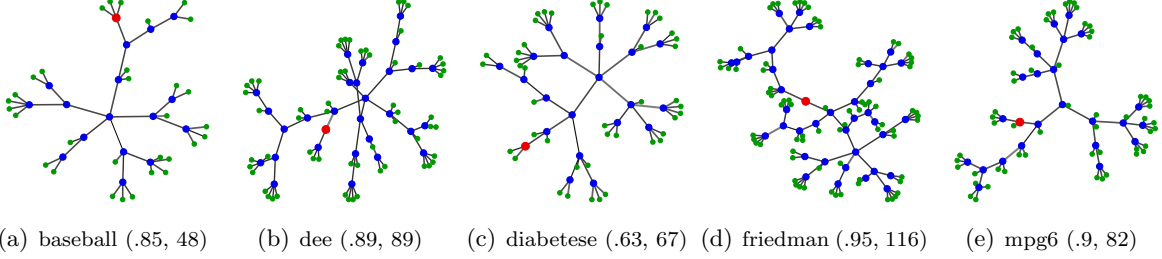


Fig. 6: Regression Trees. (a) - (e) show best performing tree structure of the respective dataset, their accuracy and tree size shown in brackets. The red node in a tree is the root node (output node), function nodes are blue, and leaf nodes are green. The link connecting nodes are neural weights.

1 **BNeuralT pattern recognition (MNIST) models summary.** RMSprop optimizer was
 2 found robust and converging fastest for classification models (cf. Sec. 5.3). Hence, we train
 3 BNeuralT on the MNIST character classification dataset (LeCun et al., 2020) using RMSprop.
 4 We fed BNeuralT with pixels of MNIST character images since we do not use convolution in
 5 BNeuralT. We aimed at generating varied BNeuralT models with varied trainable parameters
 6 length by varying tree size. We hoped that a low complexity (few parameters) BNeuralT model
 7 would perform competitively with a few reported state-of-the-art. Therefore, we compare BNeu-
 8 ralT performance to gauge its robustness not only on learning small-scale problems reported in
 9 Table 2 but on large-scale learning problems like MNIST. Table 4 summarizes BNeuralT models
 10 compared with the performances of tree-based state-of-the-art classification algorithms.

11 Table 4 presents MNIST (pixels) results compared with classification trees. BNeuralT performs
 12 the best among the reported trees that work on MNIST (pixels) for character classification.
 13 However, convolution of images has been proven efficient for image classification problems. For
 14 example, CapsNet (Sabour et al., 2017), a state-of-the-art algorithm on MNIST (convolution),
 15 has an error rate of 0.25, but it uses *8 million parameters*. Compared to that, a BNeuralT on
 16 MNIST (pixels) used *23,835 trainable parameters* for an error rate of 6.08, and another model
 17 used *241,999 trainable parameters* for an error rate of 5.19. Obviously, there is a trade-off
 18 between the model’s parameters size and accuracy. The performances of a varied range of other
 19 algorithms on MNIST dataset are available at (LeCun et al., 2020). Our goal is to use as much
 20 compact model as we can for high accuracy.

21 In our few trials, BNeuralT does perform competitively with many state-of-the-art (cf. Table 4).
 22 The performance of BNeuralT is better than tree-alternating optimization (TAO) (Carreira-
 23 Perpinan and Tavallali, 2018), CART (Breiman et al., 1984), C5.0 (Quinlan, 1993), oblique
 24 classifier 1 (OC1) (Murthy et al., 1993), and generalized unbiased interaction detection and
 25 estimation (GUIDE) (Loh, 2014) algorithms that worked on MNIST raw pixels inputs (Zhar-
 26 magambetov et al., 2019) like BNeuralT (cf. Table 4).

27 We compare BNeuralT with biologically plausible models of Jones and Kording (2021) that

1 performed binary classification on MNIST’s two classes (class 3 and class 5). This is, however, a
 2 trivial comparison as BNeuralT works on all classes and uses sigmoidal dendritic nonlinearities,
 3 whereas Jones and Kording (2021)’s models work on binary class and use Leaky ReLU as
 4 dendritic nonlinearities. They obtained an error rate of 7.8%, 3.65%, and 8.89% respectively
 5 with 1-tree ($w = 2,047$), 32-tree ($w = 65,504$), and A-32-tree ($w = 65,504$) models. In contrast
 6 to Jones and Kording (2021)’s models, BNeuralT performs classification on all ten classes of
 7 MNIST pixels. Obviously, some classes are easier to learn than others (see Fig. 7), and training
 8 a binary classifier presents an entirely different difficulty level than a multi-class classification.
 9 However, although a one-to-one comparison is not possible in such a scenario, it may be worth
 10 noting that BNeuralT obtained an error rate of 7.74% ($w = 11,987$) and 6.08% ($w = 23,835$)
 11 on all ten classes. Therefore, the sparse stochastic structure of BNeuralT (e.g., Fig. 8) stands
 12 competitive with the models of Jones and Kording (2021).

13 Moreover, BNeuralT models show a linear relation between trainable parameters and their ac-
 14 curacy (cf. Table 4). Hence, BNeuralT models with relatively higher parameters and exhaustive
 15 hyperparameter tuning are able to produce efficient results. Fig. 7 shows an example BNeuralT
 16 (20K) model’s training convergence and MNIST character classification performance on a re-
 17 ceiver operating characteristic curve plot, where BNeuralT (20K) model for all classes produces
 18 a very *high sensitivity* (true-positive rate) and *very low specificity* (low false-positive rate). Of
 19 all classes, we may arrange classes on the scale of hardness of learnability in the order of “easiest
 20 to hardest” to learn as $c1, c6, c0, c7, c5, c4, c9, c2, c3$, and $c8$ (cf. Fig. 7).

21

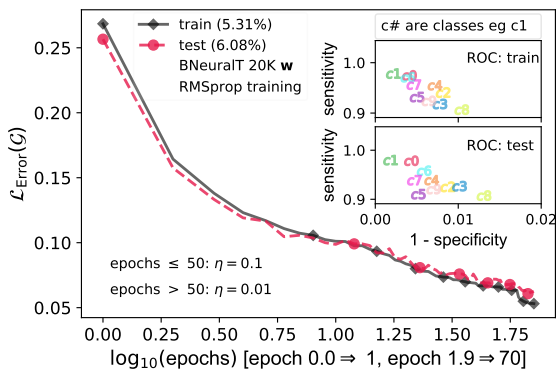


Fig. 7: BNeuralT-20K (23,835 trainable parameters w) model’s RMSprop training and test error over 70 epochs on the MNIST dataset. Zoom-in for BNeuralT performance on receiver operating characteristic curve plots on training (*inner top*) and test (*inner bottom*) sets.

Table 4: Test error % of ad hoc BNeuralT (\mathcal{G}) models with a varied number of trainable parameters on the MNIST dataset. All models are trained for 70 epochs, and where denoted \dagger is for 25 epochs. The decision tree models are reported in (Zharmagambetov et al., 2019).

	Algorithms	Error(%)
BNeuralTs	BNeuralT-10K (pixels)	7.74
	BNeuralT-18K (pixels)	6.58
	BNeuralT-20K (pixels)	6.08
	BNeuralT-200K \dagger (pixels)	5.19
Classification Trees	GUIDE (pixels, oblique split)	26.21
	OC1 (pixels, oblique split)	25.66
	GUIDE (pixels)	21.48
	CART-R (pixels)	11.97
	CART-P (pixels)	11.95
	C5.0 (pixels)	11.69
	TAO (pixels)	11.48
	TAO (pixels, oblique split)	5.26

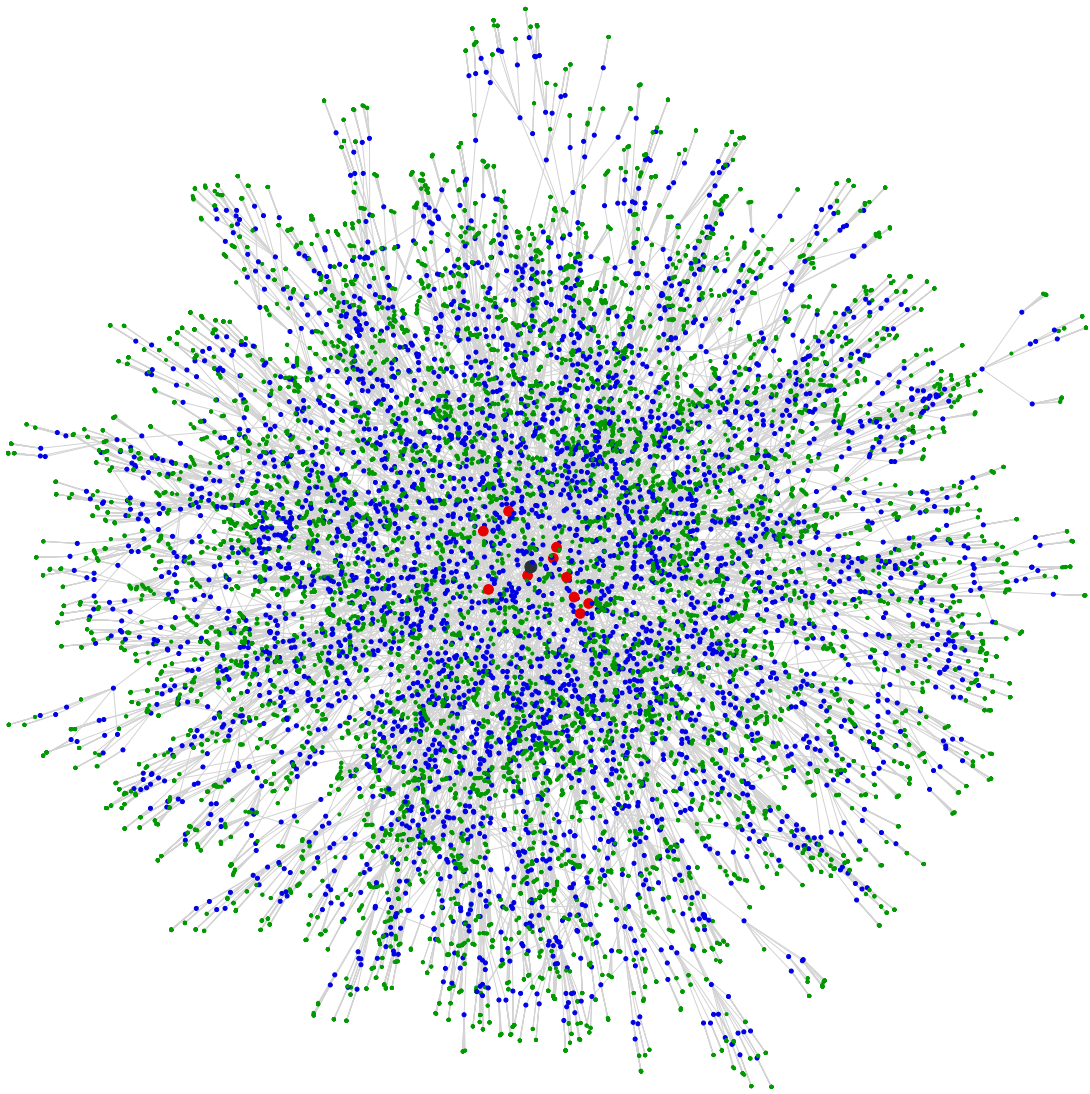


Fig. 8: BNeuralT-20K (pixels) MNIST model (tree structure). This model has 3,664 function nodes (blue nodes), 16,507 leaf nodes (green nodes), and ten class nodes (red nodes in the inner circle), and the root node (in black) in the center. This model has 6,738 edges (gray lines connecting nodes). These lines also represent neural weights. Each blue node also has its bias. Edge weights and bias together make 23,835 tree's trainable parameters. This model has a test accuracy of 94% (an error rate of 6.08%).

1 **5.3 BNeuralT convergence analysis**

2 We evaluated average asymptotic convergence profiles of all six SGD optimizers for optimizing
3 BNeuralT on classification and regression problems (cf. Figs. 9, 10, and 11). For such an
4 analysis, we recorded training and test accuracies of each training epoch. Since we ran algorithms
5 for 30 independent instances, we analyzed the average trajectory of all 30 runs. In each run, an
6 ad hoc BNeuralT architecture was generated, which could vary in tree size between a minimum
7 “outputs $\times 2$ ” nodes to a maximum $(m^{p+1}-1)/(m-1)$ nodes. Hence, BNeuralT architecture and
8 trainable parameters varied stochastically at each instance of the experiment. Such high entropy
9 network architectures pose difficulties for SGDs to perform well consistently. We, therefore,
10 investigated BNeuralT models’ accuracy against their architecture (number of parameters) (cf.
11 Fig. 12).

12 **BNeuralT classification models convergence.** Fig. 9 shows convergence (training and
13 test errors) profiles of ES training of BNeuralT having *sigmoid* nodes, 0.1 learning rate, and
14 0.4 leaf generation rate. With this BNeuralT’s setting, we observe that BNeuralT’s RMSprop
15 converges the fastest among all SGDs. RMSprop also outperformed all other optimizers. NAG
16 and MGD were asymptotically closer to RMSprop optimizer. Like RMSprop, NAG and MGD
17 showed monotonically increasing training convergence. However, on the test sets, we observe
18 that the models started overfitting. This motivated us to use early-stopping with restore best.
19 Adagrad showed the most interesting convergence profile as initially, it had worse convergence
20 among all optimizers, and while approaching higher epochs, it started rapidly improving its
21 convergence. Thus, over an asymptotic behavior, Adagrad converged to a similar accuracy to
22 that of RMSprop’s accuracy. The optimizers NAG and MGD behave equivalently. Adam and
23 GD were found sensitive to BNeuralT architecture (and trainable parameters).

24 **BNeuralT regression models convergence.** Fig. 10 shows convergence (training and test
25 errors) profiles of ES training of BNeuralT having *sigmoid* nodes, 0.1 learning rate, and 0.4 leaf
26 generation rate. The convergence profiles of optimizers on five regression problems suggest that
27 RMSprop and Adagrad were better converging optimizers. Similar to its classification prob-
28 lems profile, RMSprop converged faster than other optimizers for regression problems. Adagrad
29 showed slower convergence than RMSprop. However, unlike its performance on classification
30 problems, Adagrad showed a more stable convergence profile for regression. Contrary to classifi-
31 cation problems, overfitting occurred only occasionally for regression problems when comparing
32 training and test convergence profiles.

33 **BNeuralT and MLP settings convergence.** In Fig. 11, we compare convergence of six
34 optimizers for optimizing both BNeuralT and MLP on various settings. We show this comparison
35 on “glass” and “miles per gallon” datasets as an example. (Supplementary shows convergence of
36 all other datasets on various settings.) In Fig. 11, we observe that the learning rate 0.1 produces
37 stable convergence for all optimizers. For learning rate 0.1, Adam does not converge as good as

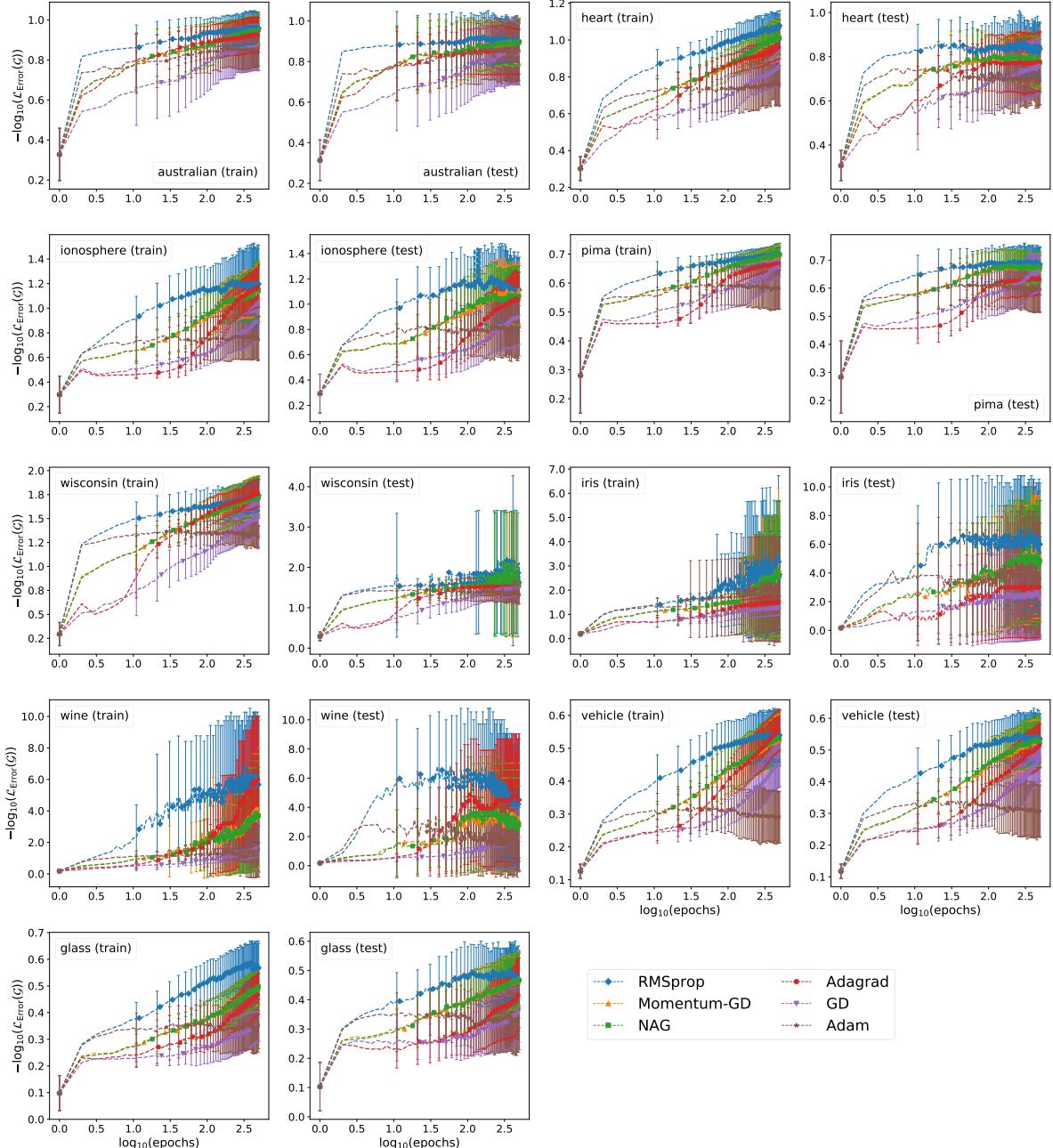


Fig. 9: Early-stopping training of BNeuralT having *sigmoid* nodes, 0.1 learning rate, and 0.4 leaf generation rate. BNeuralT average convergence trajectory performance computed over 30 independent runs for six optimizers over nine classification problems. The x-axis, $\log_{10}(\text{epochs})$ has the range [0.0, 2.7] and is the training epochs 1 to 500. The y-axis, $-\log_{10}(L_{\text{Error}}(\mathcal{G}))$ has the range [0, 10] and is the log scale of the training and test accuracies. An error of 0.01 (accuracy 99%) on the $-\log_{10}(L_{\text{Error}}(\mathcal{G}))$ scale has a value of 2.0 and an accuracy of 90% has a value of 1.0. Thus, a higher value on the y-axis is better. Error bar is the standard deviation of $-\log_{10}(L_{\text{Error}}(\mathcal{G}))$ and it indicates stochasticity of the convergence that helps an optimizer escape local minima better. Thus, a larger length is better. For each data, training and test convergence pair are plotted for 500 epochs (on the log scale, 2.7). RMSprop, MGD, NAG, Adagrad, GD, and Adam are respectively indicated in blue, orange, green, red, purple, and brown colors, respectively, with symbols diamond, triangle, circle, downward triangle, and star.

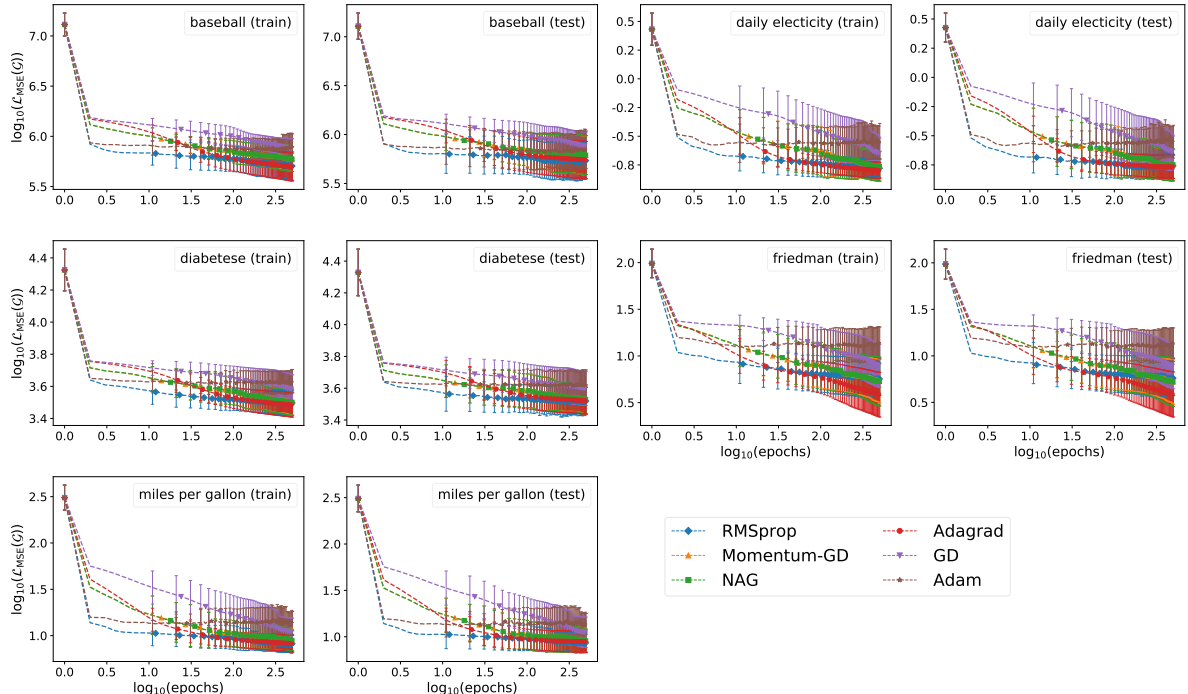


Fig. 10: BNeuralT average convergence trajectory performance computed over 30 independent runs for six optimizers over five regression problems. The x-axis, $\log_{10}(\text{epochs})$ has the range [0.0, 2.7] and is the training epochs 1 to 500. The y-axis, $\log_{10}(\mathcal{L}_{\text{MSE}}(\mathcal{G}))$ is the training and test sets mean square error (MSE) on the log scale. An MSE 0.01 on the log scale has a value of -2.0 . Thus, a lower value is better. Error bar is the standard deviation of $\log_{10}(\mathcal{L}_{\text{MSE}}(\mathcal{G}))$ and it indicates stochasticity of the convergence that helps an optimizer escape local minima better. Thus, a larger length is better. For each dataset, training and test convergence pair are plotted for 500 epochs (on the log scale, 2.7). The optimizers RMSprop, MGD, NAG, Adagrad, GD, and Adam are respectively indicated in blue, orange, green, red, purple, and brown colors with respective symbols diamond, triangle, circle, and star.

1 other algorithms (cf. Figs. 11(a) and 11(d)). However, Adam does converge when learning rate
2 is 0.001 (cf. Figs. 11(b), 11(e), 11(h), and 11(k)). For learning rate 0.001, Adagrad does not
3 converge as good as others. It may be observed that Adagrad’s adaptively decreasing learning
4 rate property made the convergence very slow and it may require more epochs to converge (cf.
5 Figs. 11(b), 11(e), 11(h), and 11(k)).

6 **Convergence of optimizers on ReLU.** For *ReLU* activation function, Adagrad and GD being
7 the slowest converging optimizers performed better than other faster converging optimizers like
8 RMSprop, Adam, and NAG (cf. Figs. 11(c), 11(f), 11(l) and 11(l)). In fact, when using *ReLU*
9 activation function for regression problems, BNeuralT suffered from exploding gradient issues
10 when using optimizers like GD, MGD, NAG, and Adam during some instances of runs of some
11 datasets. Adagrad, however, remained unaffected by exploding gradient issue. This is due to
12 its decreasing convergence speed. BNeuralT’s performance with *ReLU*, due to its high sparsity,
13 was affected by exploding gradient effect more than the MLP, which showed more tolerance to
14 exploding gradient effect due to its large number of parameters (cf. Supplementary Fig. A3).

15 **Convergence of accuracy against trainable parameters.** BNeuralT’s tree size (proportional
16 to trainable parameter) and test accuracy in Fig. 12 suggest that RMSprop compared
17 to other optimizers can optimize ad hoc structure better. We observed that the accuracy of
18 BNeuralT increases with increasing tree size. However, accuracy dropped for some outliers
19 in the connected scatter plot in Fig. 12. This was because many points were within a specific
20 range. For classification problems, except for RMSprop, NAG was another better optimizer. For
21 regression problems, along with RMSprop, Adagrad was another better performing optimizer.
22 BNeuralT’s RMSprop optimizer showed rather more stable performance for stochastically vary-
23 ing architectures compared to other optimizers. For the pattern recognition MNIST dataset,
24 RMSprop optimizer was used, and it showed a linear increase in accuracy for increasing order
25 of tree size.

26 6 Discussion

27 We designed and investigated a learning system called BNeuralT capable of solving three classes
28 of machine learning problems: classification, regression, and pattern recognition. We assessed
29 the capability of this neural tree algorithm as a single neuron model approximating computa-
30 tional dendritic tree-like behavior (cf. Figs. 2 and Fig. 4). This algorithm can also be considered
31 a highly sparse NN trained using SGD optimizers. To train BNeuralT using SGDs, we de-
32 signed a recursive backpropagation algorithm. Therefore, we broadly assessed three aspects of
33 a learning system, i.e., its performance on (i) stochastically generated highly sparse models, (ii)
34 sigmoid and *ReLU* functions and their dendritic interactions with internal nodes, and (iii) opti-
35 mizers asymptotic convergence behavior. We had a diverse range of classification and regression
36 problems and algorithms to compare BNeuralT’s capabilities over these dimensions.

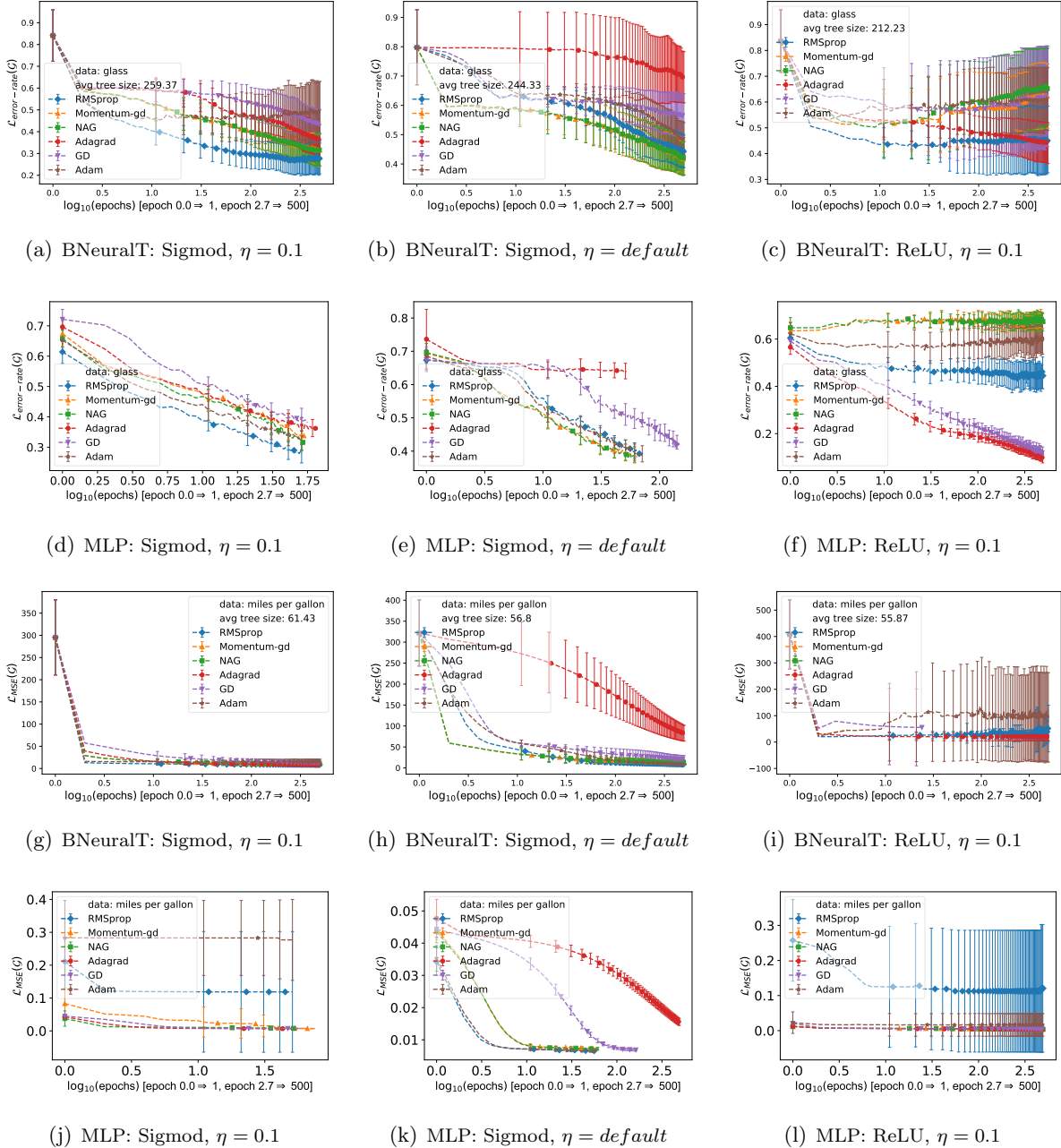


Fig. 11: Comparison of convergence of optimizers for optimizing BNeuralT and MLP and optimizers convergence over varied learning rate settings and activation function usage. (a)–(f) Classification problem where y-axis is an error rate. (g)–(l) Regression problems where y-axis is an MSE. The x-axis, $\log_{10}(\text{epochs})$ has the range $[0.0, 2.7]$ and is the training epochs 1 to 500. For MLP, early-stopping method show values for optimizes only upto the epochs where training stopped. Learning rate η value *default* indicates that RMSprop, Adam, and Adagrad has a value of 0.001 as their learning rate and GD, NAG, and MGD has a value of 0.01.

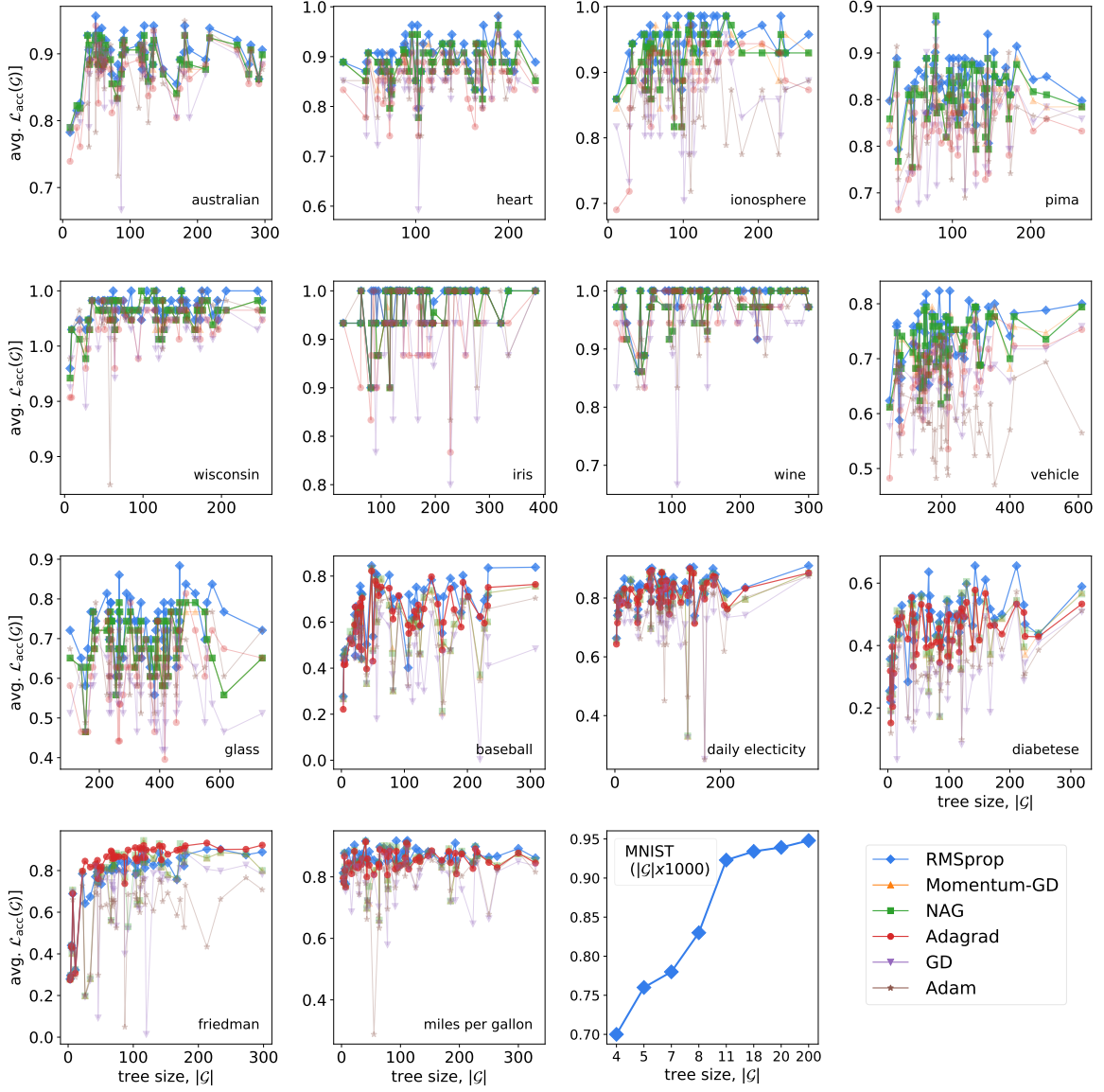


Fig. 12: BNeuralT model’s tree size $|\mathcal{G}|$ (x-axis) compared with its average (avg.) accuracy $\mathcal{L}_{\text{acc}}(\mathcal{G}) = (1 - \mathcal{L}_{\text{Error}}(\mathcal{G}))$ (y-axis has range $[0, 1]$) on the training sets of nine classification problems, five regression problems, and one pattern recognition problem. For the pattern recognition problem, BNeuralT model’s tree size $|\mathcal{G}|$ (x-axis) is in the multiple of 1000. The optimizers RMSprop, MGD, NAG, Adagrad, GD, and Adam are respectively indicated in blue, orange, green, red, purple, and brown colors, with symbols diamond, triangle, circle, downward triangle, and star. For a few cases, convergence is linear to tree size, however for a few, high accuracy is achieved with smaller trees. For MNIST, RMSprop has 10-epoch of stochastic online training and shows a linear relation with tree size. In all tasks, the convergence of RMSprop (blue diamonds) is the best, followed by NAG (green squares) and MGD (yellow triangles). Adagrad (red circles) shows competitive performance with RMSprop (blue diamonds) for regression problems. Classification datasets have green and blueish hues because NAG and RMSprop are top optimizers, and for regression datasets, plots appear to be red and blueish hue because of RMSprop and Adagrad are top optimizers.

Since BNeuralT resembles a highly sparse NN, its performance was assessed against MLP (and MLP with dropout rate similar to the probability of keeping nodes in BNeuralT) for their similar versions of SGD training. Six classification trees of BNeuralT, among all other algorithms and experiments, were top-performing models with a very low number of parameters. In fact, BNeuralT performed better against MLP dropout on classification problems, and it statistically had a similar performance on regression problems. This BNeuralT’s performance against MLP’s dropout regularization technique confirms that SGD training of any *a priori* arbitrarily “thinned” network has the potential to solve machine learning tasks with equivalent or better degree of accuracy than a fully connected symmetric and systematic NN architecture.

We used six different SGD optimizers for optimizing BNeuralT and MLP. Each optimizer behaved differently in terms of their asymptotic convergence depending on what problem they solve, how their learning rate behaved over the training epochs, and what activation function was used (cf. Figs. 9, 10, and 11). For example, with a 0.1 learning rate, RMSprop was the best among others for BNeuralT optimization over classification problems. For regression problems, both RMSprop and Adagrad performed well. Adagrad, however, was slow on classification problems. Since optimizers had to optimize the same architecture in an instance, it may be the continuous-variable output in the case of regression problems has helped Adagrad perform better than the discrete variable output in classification problems.

The use of activation functions influenced the performances of SGD optimizers. The sigmoid function proved to be more efficient with RMSprop, NAG, and MGD. Whereas ReLU proved to be efficient with Adagrad. This may be related to Adagrad’s slow convergence speed that avoided weights to explode too quickly compared to faster converging optimizers like RMSprop (cf. Fig. 11(a-b), 11(d-e), 11(g-h)). This phenomenon of Adagrad may be confirmed since GD being the slowest converging SGD, was also found efficient when ReLU is used (cf. Fig. 11(c, f, and e)). Additionally, Adagrad converged better with a learning rate of 0.1 than 0.001 (e.g. Fig. 11(a-b)). This is because Adagrad was too slow at earlier epochs that prevented it from converging within a fixed number of training epochs.

BNeuralT is operationally similar to HFNT and MONT algorithms. The HFNT and MONT algorithms model structures were genetically optimized as opposed to BNeuralT structure. The better performance of BNeuralT compared to HFNT and MONT shows that the stochastic structure of BNeuralT has a high potential to solve machine learning problems (cf. Table 2). However, this performance comparison also shows that BNeuralT models can be further compacted because both HFNT and MONT on classification problems had smaller average tree sizes than BNeuralT. This confirms that optimization of structure made HFNT and MONT more compact, although their accuracies were slightly compromised. On regression problems, however, BNeuralT performed better than HFNT both in terms of tree size and regression fit.

BNeuralT’s performance compared to MLP’s (with and without dropout) models and genetically

1 optimized HFNT and MONT models confirms *Occam’s razor principle of parsimony* for machine
2 learning model selection that the simple models possess better generalization capability than the
3 complex models (Blumer et al., 1987). Indeed, it is similar to the *sparsity of the biological brain*
4 that a sparse network generalizes better or as good as a dense network (Friston, 2008; Herculano-
5 Houzel et al., 2010; Hoefer et al., 2021). Moreover, it has been argued that a dense network is
6 often overparameterized, and only a minute fraction of it is required for generalization (Denil
7 et al., 2013). Our result is in a similar line because BNeuralT, with only an average of 222
8 parameters, which is *only* 13.5% of parameters than that of MLP’s average 1638 parameters,
9 is able to generalize machine learning problems better or with similar accuracy than MLP.
10 Additionally, the sparsity and compactness of BNeuralT models reduce memory usage and CO₂
11 footprint as they require less memory and computational resources than dense networks.

12 The decision tree algorithms DT and RF (ensemble of DTs) computationally have dedicated
13 paths from the root to leaves (Breiman et al., 1984; Breiman, 2001). BNeuralT computationally
14 also has dedicated information processing paths but from leaves to root. Although these
15 algorithms differ in how nodes propagate information, a performance comparison suggests that
16 BNeuralT has superior or competitive performances compared with DT and RF (cf. Table 2).
17 This performance is noticeable since RF is an ensemble algorithm that, using bootstrapping,
18 combines 100 DTs to construct a predictor (Breiman, 2001). Hence, the better performance of
19 a standalone randomly generated BNeuralT model shows its high capabilities. Especially when
20 RF being an ensemble of many trees, is more complex than a small and compact BNeuralT tree.
21 Moreover, DTs are symbolic machine learning algorithms whose models offer inference ability as
22 opposed to the black-box nature of NNs because of their ability to induce data using dedicated
23 paths from the root to leaves. Likewise, BNeuralT has dedicated information processing paths
24 from leaves to root, and such paths related to particular subsets of inputs may be analyzed,
25 which potentially may offer inference ability to BNeuralT (cf. Figs. 5 and 6). Thus, BNeuralT
26 models are potentially inferable as opposed to NNs. However, this is a challenging task since
27 BNeuralT’s nodes combine inputs and perform a nonlinear or linear transformation.

28 We assessed BNeuralT performance against GP, NBC, and SVM. These three algorithms take
29 Gaussian kernels. That is, these algorithms have a powerful approach towards prediction. GP
30 and NBC algorithms are robust and powerful algorithms if input data follow a normal distribu-
31 tion. Similarly, SVM uses Gaussian kernels to project input to high dimensions, increasing the
32 separability of data points to help to classify them (Cortes and Vapnik, 1995). Better perfor-
33 mance of BNeuralT compared to these algorithms on classification and regression problems (cf.
34 Table 2) suggests that BNeuralT offers an efficient alternative to these algorithms as BNeuralT
35 does not make any assumption about data to generate a hypothesis (model) when fitting or
36 classifying data.

37 The biologically plausible design of BNeuralT comes from its structural arrangement that takes

random repeated input and has a computational dendritic tree-like organization with sigmoidal nonlinearities or ReLU linearity through its internal nodes (London and Häusser, 2005). The biologically plausible computational dendritic tree-like models 1-tree and 32-tree have a regular structural arrangement where repeated inputs are fed to a neuron systematically to form a tree structure (Jones and Kording, 2021). Whereas BNeuralT takes randomly generated inputs and takes a non-systematic stochastic approach to its tree construction (cf. Fig. 2). Moreover, BNeuralT works on multi-class classification; and 1-tree, 32-tree, and A-32-tree models work on binary classification (Jones and Kording, 2021).

BNeuralT’s comparison with 1-tree, 32-tree, A-32-tree models, although limited, presents a noticeable performance. The error rate of BNeuralT on the MNIST dataset on all ten classes classification was 6.08% with 23835 parameters. The error rates of 1-tree, 32-tree, A-32-tree models on the binary classification of classes 3 and 5 of the MNIST dataset were reported as 7.8%, 3.65%, and 8.89%, respectively, and they had 2047, 65504, 65504 parameters, respectively. This result confirms BNeuralT’s potential to produce capable learning systems, especially when BNeuralT’s structural randomness (cf. Fig. 2) is closer to the randomness of biological computational dendritic-tree (Travis et al., 2005).

7 Conclusions

We propose a new algorithm Backpropagation Neural Tree (BNeuralT). Our BNeuralT algorithm plausibly has a *biological dendritic tree-like* modeling capability. It has a *single neuron-like* model with sigmoidal dendritic nonlinearities or rectified linear unit (ReLU) based dendritic linearity. It uses random repeated inputs at the leaves of subtrees attached to a single neuron, which is the root of a tree. BNeuralT uses stochastic gradient descent (SGD) optimizers to optimize stochastically generated sparse tree structures that are potentially minimal subsets of neuron networks (NNs). We propose a *recursive error backpropagation algorithm* to apply SGDs to train trees that require pre-order and post-order traversal in a depth-first-search manner for their forward pass and backward pass computations.

The results showed that our stochastically generated biologically plausibly tree structure and recursive error backpropagation algorithm have the capacity to learn a wide variety of machine learning problems. Moreover, we show that any stochastically generated tree structures can learn machine learning problems with high accuracy, and structure optimization may only be required for making models more compact. However, there is a trade-off for compacting models as we found that making the models more compact means compromising on accuracy. Additionally, BNeuralT’s strong performance compared to MLP’s dropout regularization technique confirms that SGD training of any “*a priori*” arbitrarily “*thinned network*” (spares tree structures) has the potential to solve machine learning tasks with equivalent or better degree of accuracy.

1 The sigmoidal dendritic nonlinearities (sigmoid function used at tree’s root and internal nodes)
2 performed obviously better than a linear dendritic tree (sigmoid function used at tree’s root and
3 ReLU at internal nodes). However, the linear dendritic tree differed from the best performing
4 nonlinear dendritic tree by only about 10% accuracy. Nevertheless, it was comparable with a
5 few nonlinear dendritic tree models, especially with those trained with gradient descent (GD),
6 momentum GD, and Adam. This shows that *purely single node* BNeuralT models might solve
7 machine learning problems efficiently.

8 On MNIST (pixels) character classification dataset, BNeuralT, when loosely compared with
9 1-tree and 32-tree biologically plausible dendritic tree algorithms, was found competitive. More-
10 over, BNeuralT performed best among select tree-based classifiers for the classification of MNIST
11 characters. On classification and regression problems, the overall performance of BNeuralT was
12 better than some varied types of well-known algorithms: decision tree, random forest, Gaussian
13 process, naïve Bayes classifier, and support vector machine. Such a performance of BNeuralT
14 came from a minimal hyperparameter setup. Therefore, this work shows that our newly designed
15 learning algorithm generates high-performing and parsimonious (therefore sustainable) models
16 balancing the complexity with descriptive ability.

17 **Declarations**

18 Authors declare no conflicts of interest. Supplementary provides all source code and data repos-
19 itory links.

20 **References**

- 21 Bache, K. and Lichman, M. (2013), ‘UCI machine learning repository’,
22 <https://archive.ics.uci.edu/ml/index.php> (Accessed on: 01 Apr 2020).
- 23 Bengio, Y., Boulanger-Lewandowski, N. and Pascanu, R. (2013), Advances in optimizing recurrent net-
24 works, in ‘IEEE International Conference on Acoustics, Speech and Signal Processing’, IEEE, pp. 8624–
25 8628.
- 26 Beniaguev, D., Segev, I. and London, M. (2020), ‘Single cortical neurons as deep artificial neural net-
27 works’, *bioRxiv* p. 613141.
- 28 Bishop, C. M. (2006), *Pattern recognition and machine learning*, Springer.
- 29 Blumer, A., Ehrenfeucht, A., Haussler, D. and Warmuth, M. K. (1987), ‘Occam’s razor’, *Information*
30 *processing letters* **24**(6), 377–380.
- 31 Breiman, L. (2001), ‘Random forests’, *Machine Learning* **45**(1), 5–32.
- 32 Breiman, L., Friedman, J., Stone, C. J. and Olshen, R. A. (1984), *Classification and regression trees*,
33 CRC Press.

- 1 Carreira-Perpinan, M. A. and Tavallali, P. (2018), Alternating optimization of decision trees, with ap-
 2 plication to learning sparse oblique trees, in ‘Advances in Neural Information Processing Systems’,
 3 Vol. 31, Curran Associates, Inc., pp. 1211–1221.
- 4 Chang, C.-C. and Lin, C.-J. (2011), ‘LIBSVM: A library for support vector machines’, *ACM Transactions*
 5 *on Intelligent Systems and Technology* **2**(3), 1–27.
- 6 Chen, Y., Yang, B. and Abraham, A. (2007), ‘Flexible neural trees ensemble for stock index modeling’,
 7 *Neurocomputing* **70**(4-6), 697–703.
- 8 Chen, Y., Yang, B., Dong, J. and Abraham, A. (2005), ‘Time-series forecasting using flexible neural tree
 9 model’, *Information Sciences* **174**(3), 219–235.
- 10 Cortes, C. and Vapnik, V. (1995), ‘Support-vector networks’, *Machine Learning* **20**(3), 273–297.
- 11 Dean, J., Corrado, G., Monga, R., Chen, K., Devin, M., Mao, M., Ranzato, M., Senior, A., Tucker,
 12 P., Yang, K. et al. (2012), Large scale distributed deep networks, in ‘Advances in Neural Information
 13 Processing Systems’, pp. 1223–1231.
- 14 Denil, M., Shakibi, B., Dinh, L., Ranzato, M. and De Freitas, N. (2013), Predicting parameters in deep
 15 learning, in ‘Advances in Neural Information Processing Systems’.
- 16 Fan, R.-E., Chang, K.-W., Hsieh, C.-J., Wang, X.-R. and Lin, C.-J. (2008), ‘LIBLINEAR: a library for
 17 large linear classification’, *Journal of Machine Learning Research* **9**, 1871–1874.
- 18 Farhoodi, R. and Kording, K. P. (2018), ‘Sampling neuron morphologies’, *bioRxiv* p. 248385.
- 19 Friston, K. (2008), ‘Hierarchical models in the brain’, *PLoS computational biology* **4**(11), e1000211.
- 20 Hay, E., Hill, S., Schürmann, F., Markram, H. and Segev, I. (2011), ‘Models of neocortical layer 5b pyra-
 21 midal cells capturing a wide range of dendritic and perisomatic active properties’, *PLOS Computational
 22 Biology* **7**(7), e1002107.
- 23 Herculano-Houzel, S., Mota, B., Wong, P. and Kaas, J. H. (2010), ‘Connectivity-driven white mat-
 24 ter scaling and folding in primate cerebral cortex’, *Proceedings of the National Academy of Sciences*
 25 **107**(44), 19008–19013.
- 26 Hodgkin, A. L. and Huxley, A. F. (1952), ‘A quantitative description of membrane current and its
 27 application to conduction and excitation in nerve’, *The Journal of Physiology* **117**(4), 500–544.
- 28 Hoefer, T., Alistarh, D., Ben-Nun, T., Dryden, N. and Peste, A. (2021), ‘Sparsity in deep learning:
 29 Pruning and growth for efficient inference and training in neural networks’, *arXiv:2102.00554*.
- 30 Jones, I. S. and Kording, K. P. (2021), ‘Might a single neuron solve interesting machine learning problems
 31 through successive computations on its dendritic tree?’, *Neural Computation* **33**(6), 1554–1571.
- 32 Jordan, M. I. and Jacobs, R. A. (1994), ‘Hierarchical mixtures of experts and the EM algorithm’, *Neural
 33 Computation* **6**(2), 181–214.

- 1 Keel (2011), ‘KEEL dataset repository’, <https://sci2s.ugr.es/keel/datasets.php> (Accessed on: 01 Apr
2 2020).
- 3 Kennedy, J. and Eberhart, R. (1995), Particle swarm optimization, in ‘Proc. of ICNN’95-International
4 Conference on Neural Networks’, Vol. 4, IEEE, pp. 1942–1948.
- 5 Keras (2020), ‘Keras the sequential model’, https://keras.io/guides/sequential_model/ (Accessed on: 01
6 Apr 2020).
- 7 Kingma, D. P. and Ba, J. (2015), Adam: A method for stochastic optimization, in ‘3rd International
8 Conference for Learning Representations (ICLR)’.
- 9 LeCun, Y., Cortes, C. and Burges, C. J. (2020), ‘The MNIST database of handwritten digits’,
10 <http://yann.lecun.com/exdb/mnist/> (Accessed on: 01 Apr 2020).
- 11 Lee, C.-Y., Gallagher, P. W. and Tu, Z. (2016), Generalizing pooling functions in convolutional neural
12 networks: Mixed, gated, and tree, in ‘Artificial Intelligence and Statistics’, pp. 464–472.
- 13 Liu, D. C. and Nocedal, J. (1989), ‘On the limited memory BFGS method for large scale optimization’,
14 *Mathematical Programming* **45**(1), 503–528.
- 15 Loh, W.-Y. (2014), ‘Fifty years of classification and regression trees’, *International Statistical Review*
16 **82**(3), 329–348.
- 17 London, M. and Häusser, M. (2005), ‘Dendritic computation’, *Annual Review of Neuroscience* **28**, 503–
18 532.
- 19 McCulloch, W. S. and Pitts, W. (1943), ‘A logical calculus of the ideas immanent in nervous activity’,
20 *The Bulletin of Mathematical Biophysics* **5**(4), 115–133.
- 21 Mel, B. W. (2016), Toward a simplified model of an active dendritic tree, in G. Stuart, N. Spruston and
22 M. Häusser, eds, ‘Dendrites’, chapter 16, pp. 405–486.
- 23 Mitchell, T. M. (1997), *Machine learning*, McGraw-Hill.
- 24 Murthy, S., Kasif, S., Salzberg, S. and Beigel, R. (1993), OC1: A randomized induction of oblique decision
25 trees, in ‘Proc. 11th National Conference on Artificial Intelligence (AAAI)’, Vol. 93, pp. 322–327.
- 26 Ojha, V. K., Abraham, A. and Snášel, V. (2017), ‘Ensemble of heterogeneous flexible neural trees using
27 multiobjective genetic programming’, *Applied Soft Computing* **52**, 909–924.
- 28 Ojha, V. and Nicosia, G. (2020), Multi-objective optimisation of multi-output neural trees, in ‘IEEE
29 Congress on Evolutionary Computation (CEC)’, IEEE, pp. 1–8.
- 30 Pedregosa, F., Varoquaux, G., Gramfort, A., Michel, V., Thirion, B., Grisel, O., Blondel, M., Pretten-
31 hofer, P., Weiss, R., Dubourg, V. et al. (2011), ‘Scikit-learn: Machine learning in python’, *Journal of
32 Machine Learning Research* **12**, 2825–2830.
- 33 Pereira, R., Couto, M., Ribeiro, F., Rua, R., Cunha, J., Fernandes, J. P. and Saraiva, J. (2017), Energy
34 efficiency across programming languages: how do energy, time, and memory relate?, in ‘Proceedings of
35 the 10th ACM SIGPLAN International Conference on Software Language Engineering’, pp. 256–267.

- 1 Poirazi, P., Brannon, T. and Mel, B. W. (2003a), ‘Arithmetic of subthreshold synaptic summation in a
2 model ca1 pyramidal cell’, *Neuron* **37**(6), 977–987.
- 3 Poirazi, P., Brannon, T. and Mel, B. W. (2003b), ‘Pyramidal neuron as two-layer neural network’, *Neuron*
4 **37**(6), 989–999.
- 5 Qian, N. (1999), ‘On the momentum term in gradient descent learning algorithms’, *Neural Networks*
6 **12**(1), 145–151.
- 7 Quinlan, J. R. (1993), *C4.5: Programs for Machine Learning*, Morgan Kaufmann.
- 8 Rasmussen, C. E. and Williams, C. (2006), *Gaussian processes for machine learning*, MIT press.
- 9 Rios, L. M. and Sahinidis, N. V. (2013), ‘Derivative-free optimization: a review of algorithms and com-
10 parison of software implementations’, *Journal of Global Optimization* **56**(3), 1247–1293.
- 11 Rumelhart, D. E., Hinton, G. E. and Williams, R. J. (1986), ‘Learning representations by back-
12 propagating errors’, *Nature* **323**.
- 13 Sabour, S., Frosst, N. and Hinton, G. E. (2017), Dynamic routing between capsules, in ‘Advances in
14 Neural Information Processing Systems’, pp. 3856–3866.
- 15 Sakar, A. and Mammone, R. J. (1993), ‘Growing and pruning neural tree networks’, *IEEE Transactions
16 on Computers* **42**(3), 291–299.
- 17 Schmidt, M. D. and Lipson, H. (2009), Solving iterated functions using genetic programming, in ‘Proc.
18 11th Annual Conference Companion on Genetic and Evolutionary Computation Conference: Late
19 Breaking Papers’, ACM, pp. 2149–2154.
- 20 Sirat, J. and Nadal, J. (1990), ‘Neural trees: a new tool for classification’, *Network: Computation in
21 Neural Systems* **1**(4), 423–438.
- 22 Srivastava, N., Hinton, G., Krizhevsky, A., Sutskever, I. and Salakhutdinov, R. (2014), ‘Dropout: A simple
23 way to prevent neural networks from overfitting’, *Journal of Machine Learning Research* **15**(56), 1929–
24 1958.
- 25 Tanno, R., Arulkumaran, K., Alexander, D., Criminisi, A. and Nori, A. (2019), Adaptive neural trees, in
26 ‘Proc. 36th International Conference on Machine Learning (ICML)’, pp. 6166–6175.
- 27 Tieleman, T. and Hinton, G. (2012), ‘Lecture 6.5-rmsprop: Divide the gradient by a running average of
28 its recent magnitude’, *Coursera: Neural Networks for Machine Learning* **4**(2), 26–31.
- 29 Travis, K., Ford, K. and Jacobs, B. (2005), ‘Regional dendritic variation in neonatal human cortex: a
30 quantitative golgi study’, *Developmental Neuroscience* **27**(5), 277–287.
- 31 Wolpert, D. H. (1996), ‘The lack of a priori distinctions between learning algorithms’, *Neural Computation*
32 **8**(7), 1341–1390.
- 33 Zhang, B.-T., Ohm, P. and Mühlenbein, H. (1997), ‘Evolutionary induction of sparse neural trees’,
34 *Evolutionary Computation* **5**(2), 213–236.

¹ Zharmagambetov, A., Hada, S. S., Carreira-Perpiñán, M. Á. and Gabidolla, M. (2019), ‘An experimental
² comparison of old and new decision tree algorithms’, *arXiv:1911.03054* .

¹ **A Supplementary**

² Supplementary has three Sections: Sec A.1 contains URLs of source code repositories, README,
³ trained models, and links to data. Sec.A.2 offers convergence trajectories of BNeuralT and MLP.
⁴ Sec.A.3 supplements Table 2.

⁵ **A.1 Source code, scripts, pre-trained models, and data**

⁶ **A.1.1 BNeuralT Code**

⁷ BNeuralT algorithm source code repository: <https://github.com/vojha-code/BNeuralT> has
⁸ the following items, including training and evaluation entry points for re-producing results in
⁹ Table 2 and Table 4.

¹⁰ **A.1.2 MLP and Other Algorithms Code and Scripts**

¹¹ Scripts of MLP and other algorithms are available at:

¹² https://github.com/vojha-code/BNeuralT/tree/master/source_mlp_tf

¹³ **A.1.3 Pre-trained Models (of Table 2 and Table 4)**

¹⁴ Experiments produced pre-trained models and results are available at:

¹⁵ https://github.com/vojha-code/BNeuralT/tree/master/trained_models

¹⁶ **A.1.4 Data**

¹⁷ Classification and regression learning problems:

¹⁸ <https://github.com/vojha-code/BNeuralT/tree/master/data>

¹⁹ For these datasets, the exact sequence of all 30 independent runs for training and test can be
²⁰ found in models files pre-trained models.

²¹ Pattern recognition problem (MNIST): <http://yann.lecun.com/exdb/mnist/>

²² **A.2 Supplementary Figures**

²³ Figs. A1, A2, A3, A4, A5, A6, and A7 are the average training and test convergence performance
²⁴ computed over 30 independent runs for six optimizers of BNeuralT and MLP over nine
²⁵ classification and five regression datasets. The x-axis in Figs. A1, A2, A3, A4, A5, A6, and A7
²⁶ are $\log_{10}(\text{epochs})$ that has range [0.0, 2.7] and is the training epoch range [1, 500]. Optimizers
²⁷ RMSprop, MGD, NAG, Adagrad, GD, and Adam are indicated in blue, orange, green, red,
²⁸ purple, and brown, respectively, with symbols diamond, triangle, circle, downward triangle, and
²⁹ star. In each plot is labeled with the name of the dataset and set type. For example, iris (train)
³⁰ and iris (test) represent training set and test set convergence of optimizers on iris data.

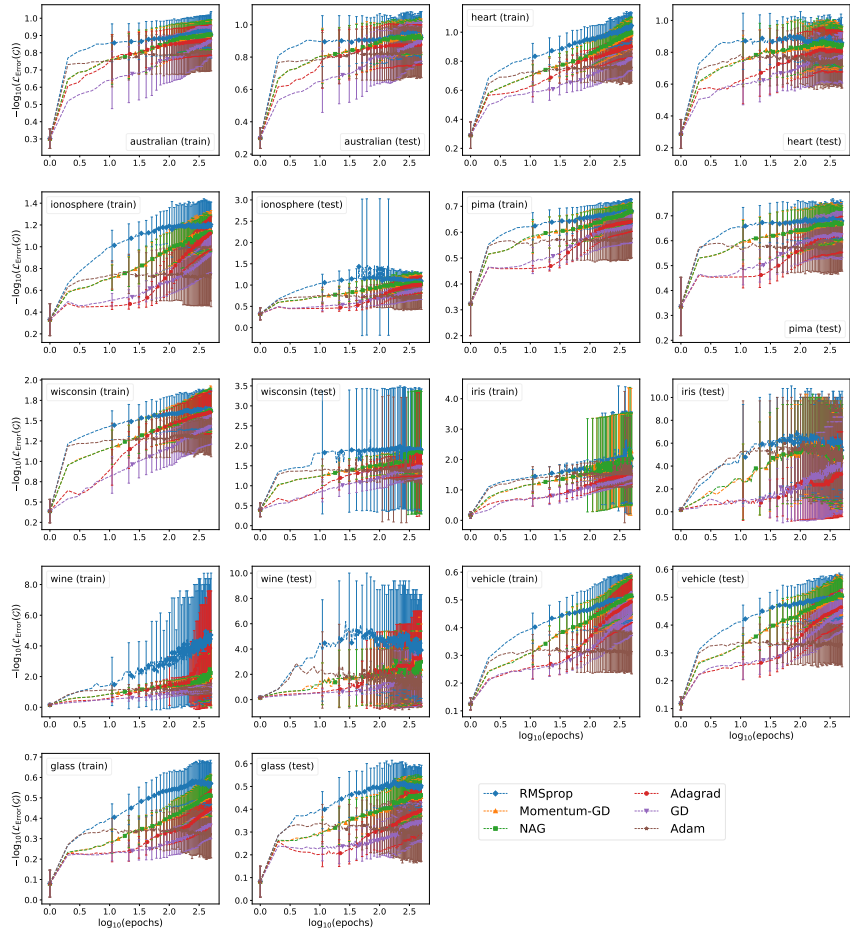
1 The performance of BNeuralT and MLP of classification problems is shown in Figs. A1(a),
2 A2(a), A3(a), A4(a), A5(a), A6(a), and A7(a). The y-axis of each plot is “ $-\log_{10}(\mathcal{L}_{\text{Error}}(\cdot))$ ”
3 that has the range [0, 10] and is the log scale of the training and test accuracies. An accuracy
4 of 99% (an error of 0.01) on $-\log_{10}(\mathcal{L}_{\text{Error}}(\cdot))$ scale has a value of 2.0, and an accuracy of 90%
5 (an error 0.1) has a value of 1.0. Thus, a *higher* value on the y-axis is better. Error bar is
6 the standard deviation of $-\log_{10}(\mathcal{L}_{\text{Error}}(\cdot))$ value. The performances of regression problems are
7 shown in Figs. A1(b), A2(b), A3(b), A4(b), A5(b), A6(b), and A7(b). The y-axis of each plot is
8 $\log_{10}(\mathcal{L}_{\text{MSE}}(\cdot))$, and it is the training and test sets MSE on the log scale. An MSE 0.01 on the
9 log scale has a value of -2. Thus, a lower value is better. Error bar is the standard deviation
10 of $\log_{10}(\mathcal{L}_{\text{MSE}}(\cdot))$. In both classification and regression plots, a larger length of error bar shows
11 higher stochasticity of an optimizer that indicates an optimizer’s higher ability to skip local
12 minima. Thus, it shows an optimizer’s better convergence ability.

13 A.2.1 BNeuralT Convergence Trajectories

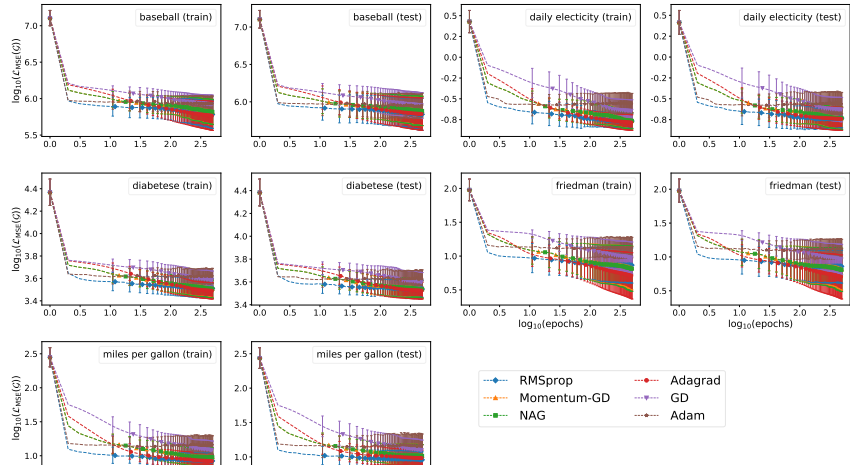
14 Figs. A1, A2, and A3 are BNeuralT models with their leaf generation rate at lower tree depth
15 set to 0.5, and they were trained with an early-stopping strategy. However, they varied in
16 the following ways: Fig. A1 has the sigmoid functions as its internal nodes. All six SGDs are
17 trained with a learning rate of 0.1. Fig. A2 has the sigmoid functions as its internal nodes. In
18 this setting, the optimizers RMSprop, Adam, and Adagrad had a learning rate of 0.001, and
19 optimizer MGD, NAG, and GD had a learning rate of 0.01. Fig. A3 has the ReLU functions as
20 its internal nodes. All six SGDs are trained with a learning rate of 0.1.

21 Figs. A1, A2, and A3 offer convergence profiles for both classification and regression problems for
22 BNeuralT setting with higher leaf generation rates, i.e., 0.5. For the higher leaf generation rate
23 (smaller model size), BNeuralT with sigmoid node and 0.1 learning rate convergence is similar
24 to the lower leaf generation rate (larger models). However, for the *default* learning rate (lower
25 learning rate), BNeuralT convergence shows a different profile (cf. Fig. A2). For a lower learning
26 rate, RMSprop (and Adam) is much slower at the beginning of training but converges very fast
27 at the reminder of the training epochs. NAG and MGD show a monotonically increasing and
28 stable learning profile. Interestingly, Adam (as evident from literature (Kingma and Ba, 2015))
29 performed the best with a learning rate of 0.001, and as shown in Fig. 9, this was not the case
30 where the learning rate was 0.1. Adam has a similar profile to RMSprop, but RMSprop produced
31 better accuracy than Adam. Adagrad, with a lower learning rate, had worse performance among
32 all six SGDs.

33 BNeuralT’s performance with *ReLU* due to its high sparsity and loss nonlinearity show a decline
34 in the model’s performance (cf. Fig. A3). In fact, it seems to suffer from exploding gradient issues
35 for some optimizers like GD, MGD, NAG, and Adam. Adagrad, however, remains unaffected
36 by this issue when the ReLU function was used.

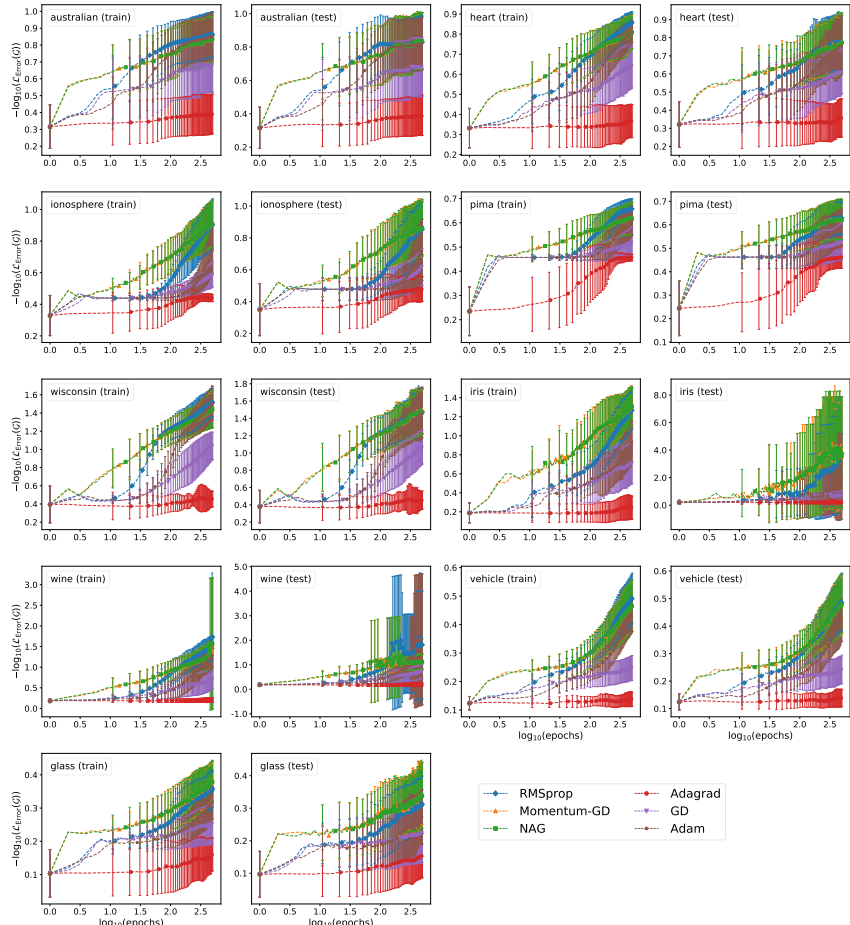


(a)

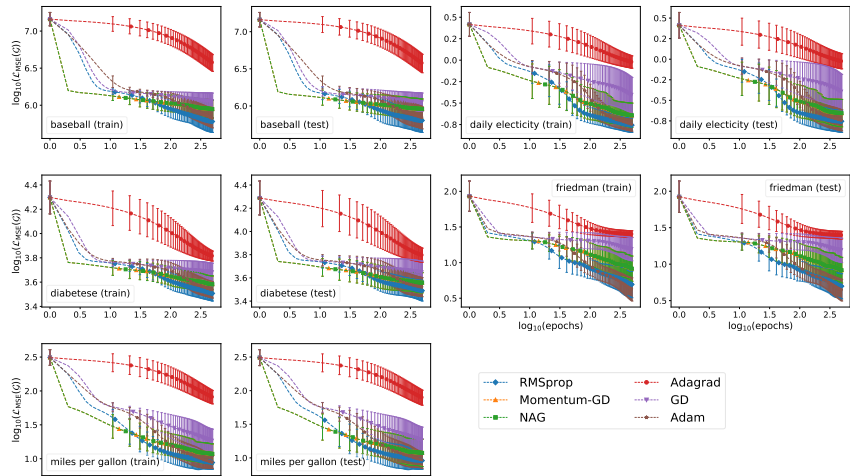


(b)

Fig. A1: BNeuralT (a) classification (b) regression models having *sigmoid* nodes, 0.5 leaf generation rate, 0.1 learning rate, and *early-stopping* strategy setting. (a) RMSprop in blue is the fastest converging optimizer as it appears at the top line in plots. Adagrad in red shows slow convergence in the beginning and only rapidly improves at higher epochs. Adam and RMSprop have similar trajectories at earlier epochs, but Adam stays at local minima. (b) Adagrad and RMSprop both appear as bottom lines in graphs showing better convergence than others.

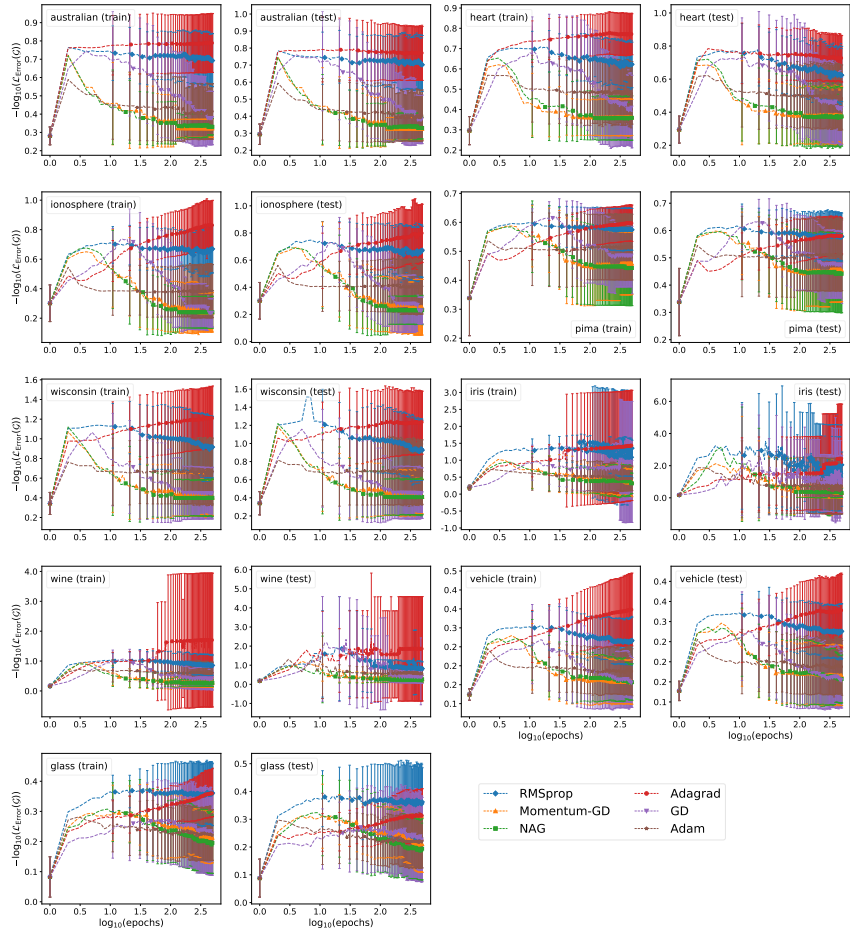


(a)

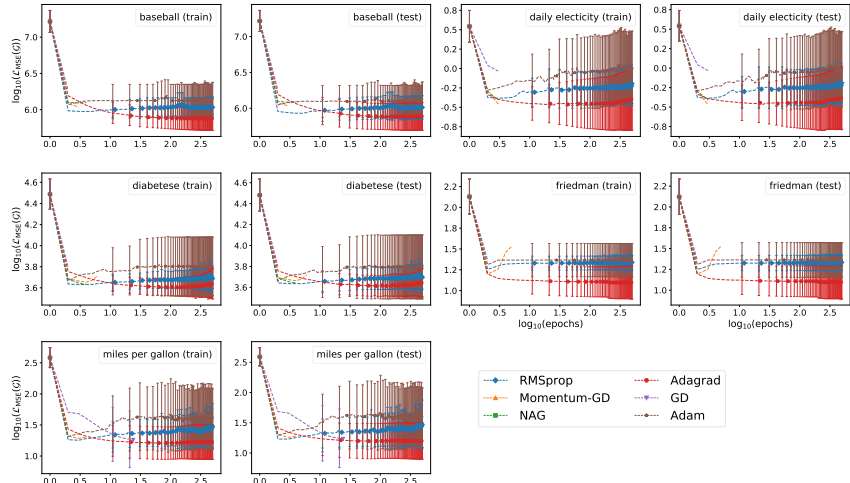


(b)

Fig. A2: BNeuralT (a) classification (b) regression models having sigmoid nodes, 0.5 leaf generation rate, *default learning rate*, and *early-stopping* strategy setting. (a) NAG in green is the fastest converging and most dominant optimizer in plots. Adagrad in red is the slowest. Adam and RMSprop have a similar trajectory, and both show rapid convergence at higher epochs. (b) RMSprop and NAG both appear as bottom lines in graphs showing better convergence than others.



(a)



(b)

Fig. A3: BNeuralT (a) classification (b) regression models having ReLU nodes, 0.5 leaf generation rate, 0.1 learning rate, and early-stopping strategy setting. (a) Adagrad in red is the fastest converging and most dominant optimizer in plots. The downward curve of other algorithms, except Adagrad, indicates that, when ReLU was used, not all structures could be trained. This is because of exploding gradient issue. This is because of exploding gradient issue. Hence the average trajectories show a downward curve (trajectory) in performance after certain epochs. This phenomenon is indicated with a sudden upward curve in plots (b) for regression. (b) Adagrad in red is the fastest converging and most dominant optimizer in plots.

¹ **A.2.2 MLP Convergence Trajectories**

- ² Figs. A4, A5, A6, and A7 are MLP algorithm settings, each with sigmoid activation functions.
³ However, they varied as per early-stopping and learning rate usage strategy: Fig. A4 was trained
⁴ with early-stopping and with a flat 0.1 learning rate for all optimizers. Fig. A5 was trained with
⁵ early-stopping, but RMSprop, Adam, and Adagrad had a learning rate of 0.001, and MGD,
⁶ NAG, and GD had a learning rate of 0.01. Fig. A6 was trained without early-stopping and with
⁷ a flat 0.1 learning rate for all optimizers. Fig. A7 was trained without early-stopping, but the
⁸ optimizers RMSprop, Adam, and Adagrad had a learning rate of 0.001 and optimizer MGD,
⁹ NAG, and GD had a learning rate of 0.01.
- ¹⁰ The convergence profiles of the optimizers for MLP were not consistent, with one optimizer
¹¹ outperforming all other optimizers across all datasets [cf. Figs. A4 (only upto ES epochs),
¹² A5 (only upto ES epochs), A6 (full epochs), and A7 (full epochs)]. RMSprop for learning
¹³ rate 0.1 performed better on four datasets. Adagrad performed relatively consistent among all
¹⁴ optimizers. Adam performed worse in cases of regression problems with a learning rate of 0.1.
¹⁵ Adam, however, does perform well with a *default* (0.001) learning rate. Adagrad shows poor
¹⁶ converges with a slower learning rate as it does in the cases of BNeuralT. NAG and MGD, in
¹⁷ the cases of both classification and regression problems, show a stable convergence profile.
- ¹⁸ Considering the convergence profiles of different optimizers on MLP training for early stopping
¹⁹ and learning rate 0.1, we observed the following: Adagrad with early stopping and higher initial
²⁰ learning rate offered better accuracy on both classification and regression problems. This is
²¹ because Adagrad's small step at higher epochs allowed networks to find a better early stopping
²² point than that of the other algorithms whose larger step size made networks converge to a
²³ premature early stopping point (cf. Figs. A4 and A6).
- ²⁴ With an initial small learning rate of 0.001, Adagrad is too slow to converge within a predefined
²⁵ number of epochs (500). In this setting, Adam seems to have an appropriate small step size to
²⁶ converge to a proper early-stopping point. The performances of RMSprop, MGD, NAG, and
²⁷ GD are next to Adam's performance (cf. Figs. A5 and A7).

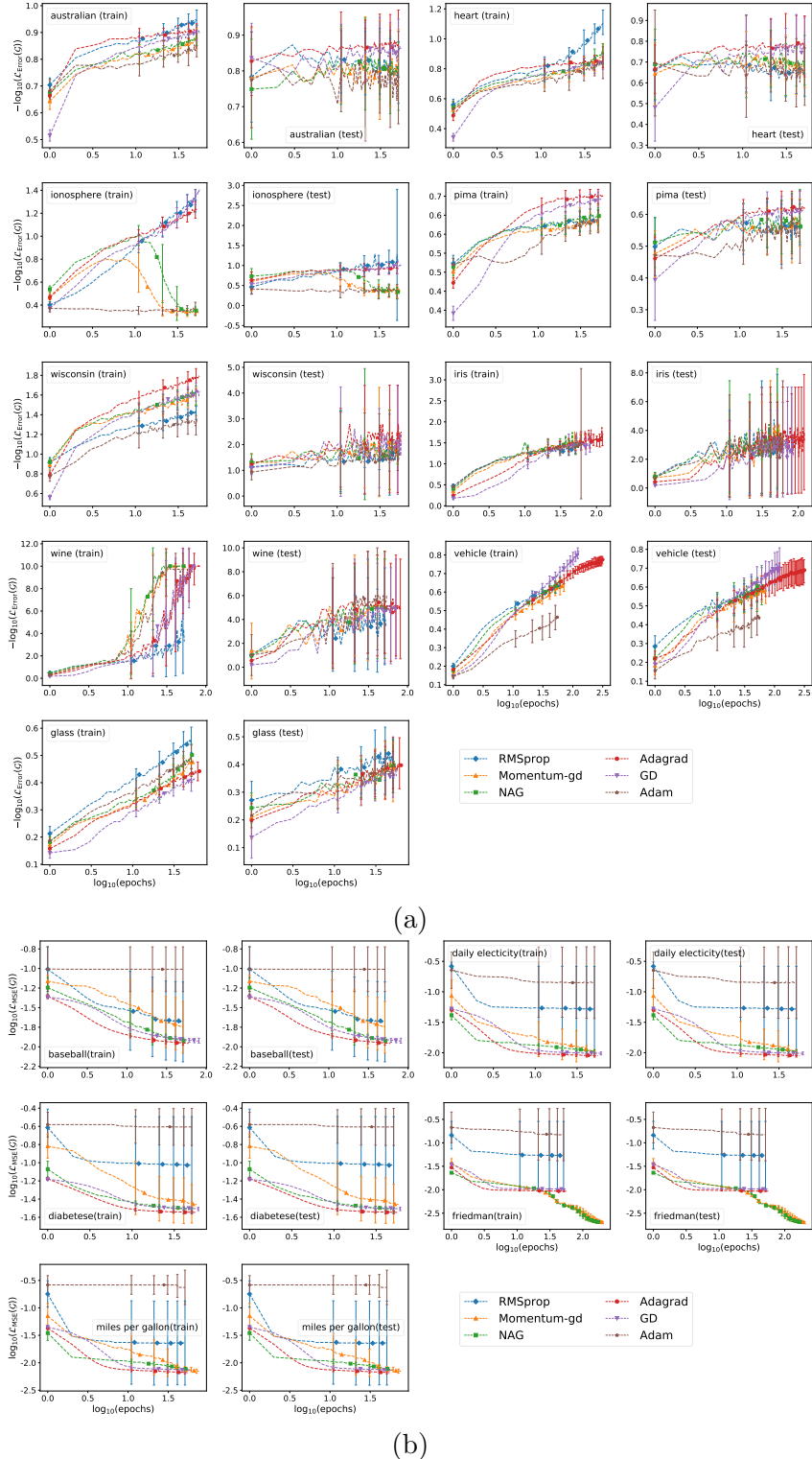


Fig. A4: MLP (a) classification (b) regression with *sigmoid* nodes trained with 0.1 learning rate and *early-stopping* strategy. (a) Adagrad in red in this setting seems taking more iteration as red lines in test sets plots show more fluctuation and longer epochs and lines are on the upper side of plots. (b) NAG is green shows better performance as lines are lower in plots.

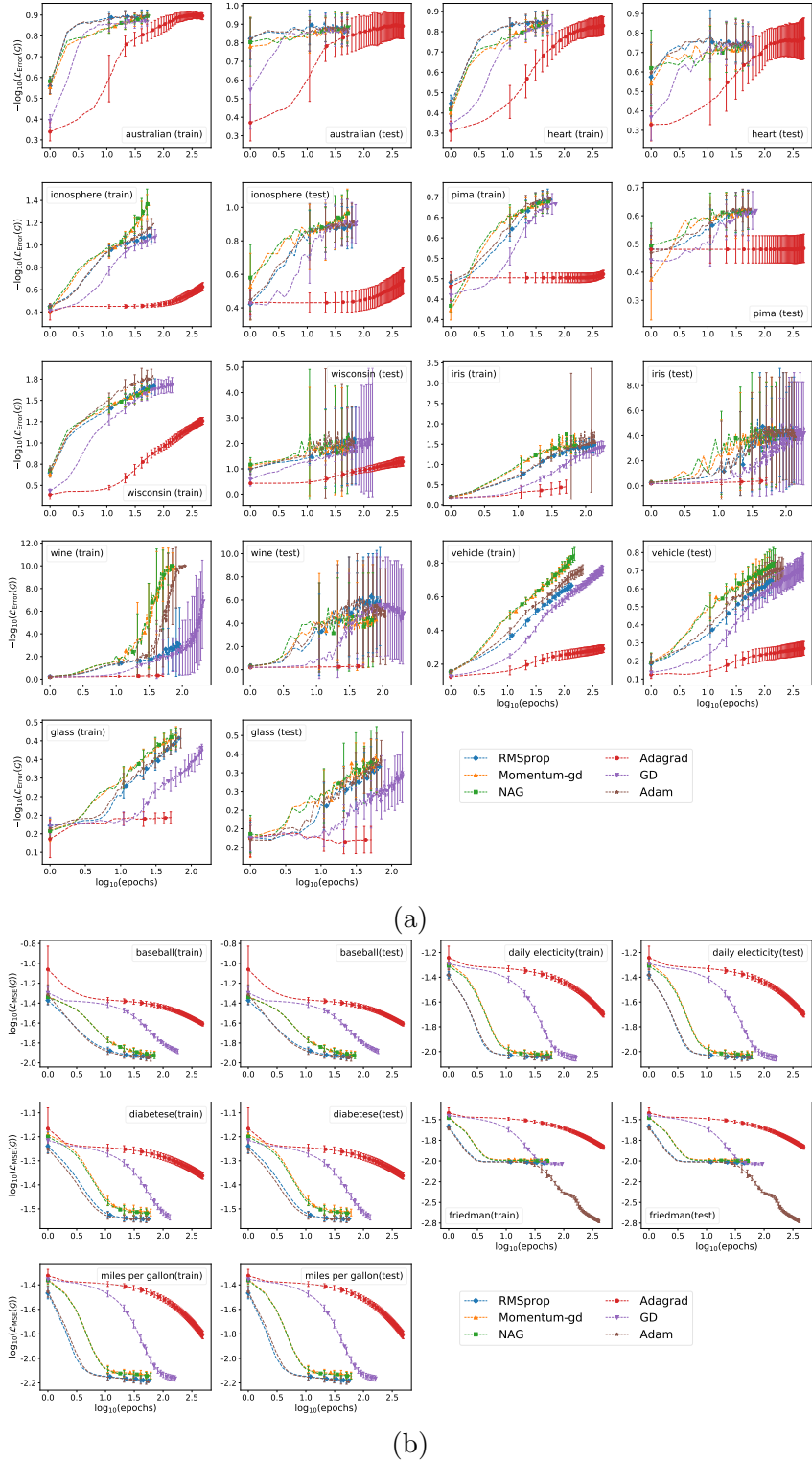


Fig. A5: MLP (a) classification (b) regression with *sigmoid* nodes trained with *default* learning rate and *early-stopping* strategy.(a) NAG and MGD, in green and orange in this setting, show better performance as on the test sets, and they are on the upper side of plots. Adam is competitively closer to NAG and MGD. (b) Adam, GD, and RMSprop in respective order show better performance as lines are lower in plots, and GD takes longer epochs to converge in early stopping.

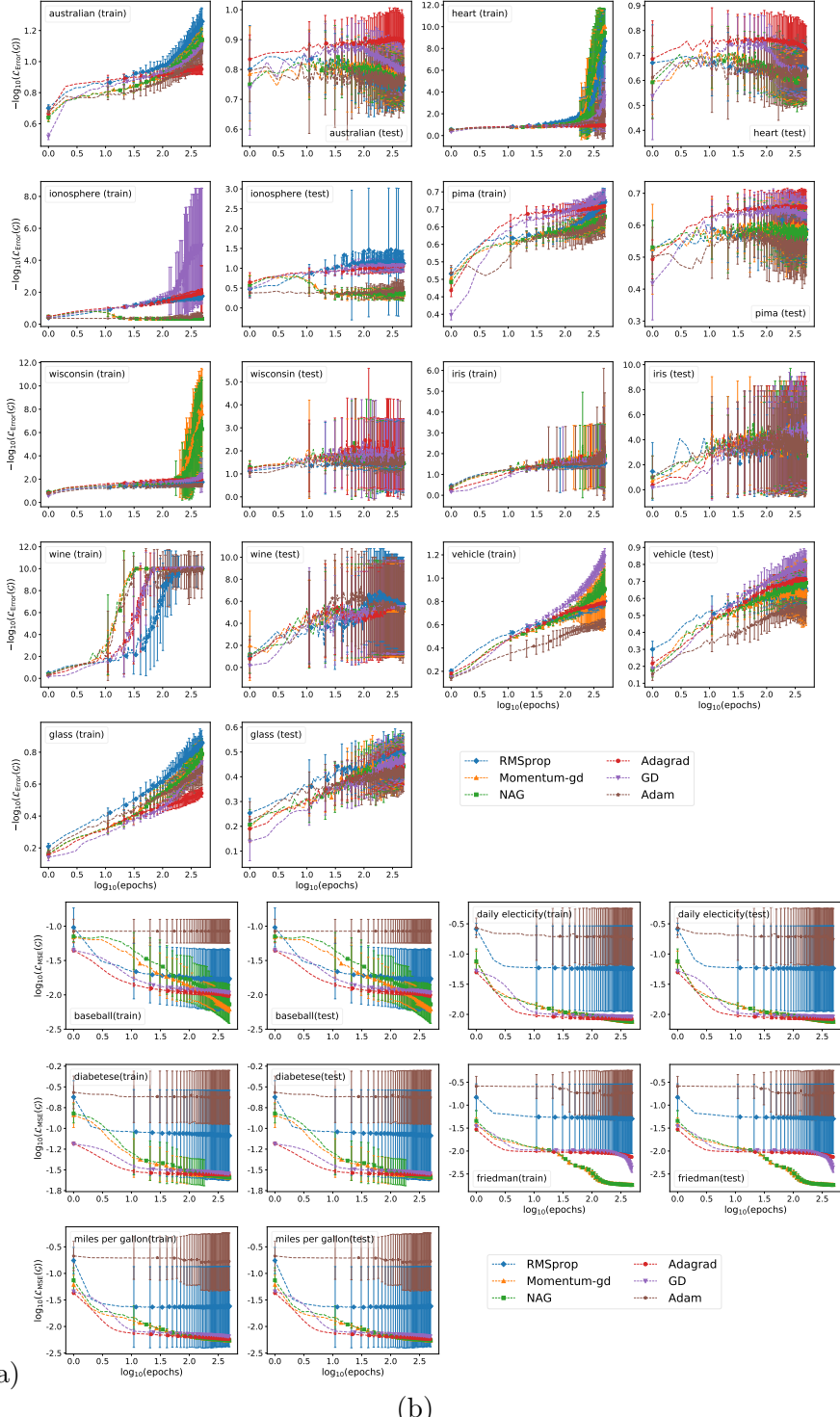


Fig. A6: MLP (a) classification (b) regression with *sigmoid* nodes trained with 0.1 learning rate and without an *early-stopping* strategy. (a) Adagrad and GD in red and purple in this setting show more fluctuation as lines are on the upper side of plots. (b) GD and NAG in purple and green show better performance as lines are lower in plots.

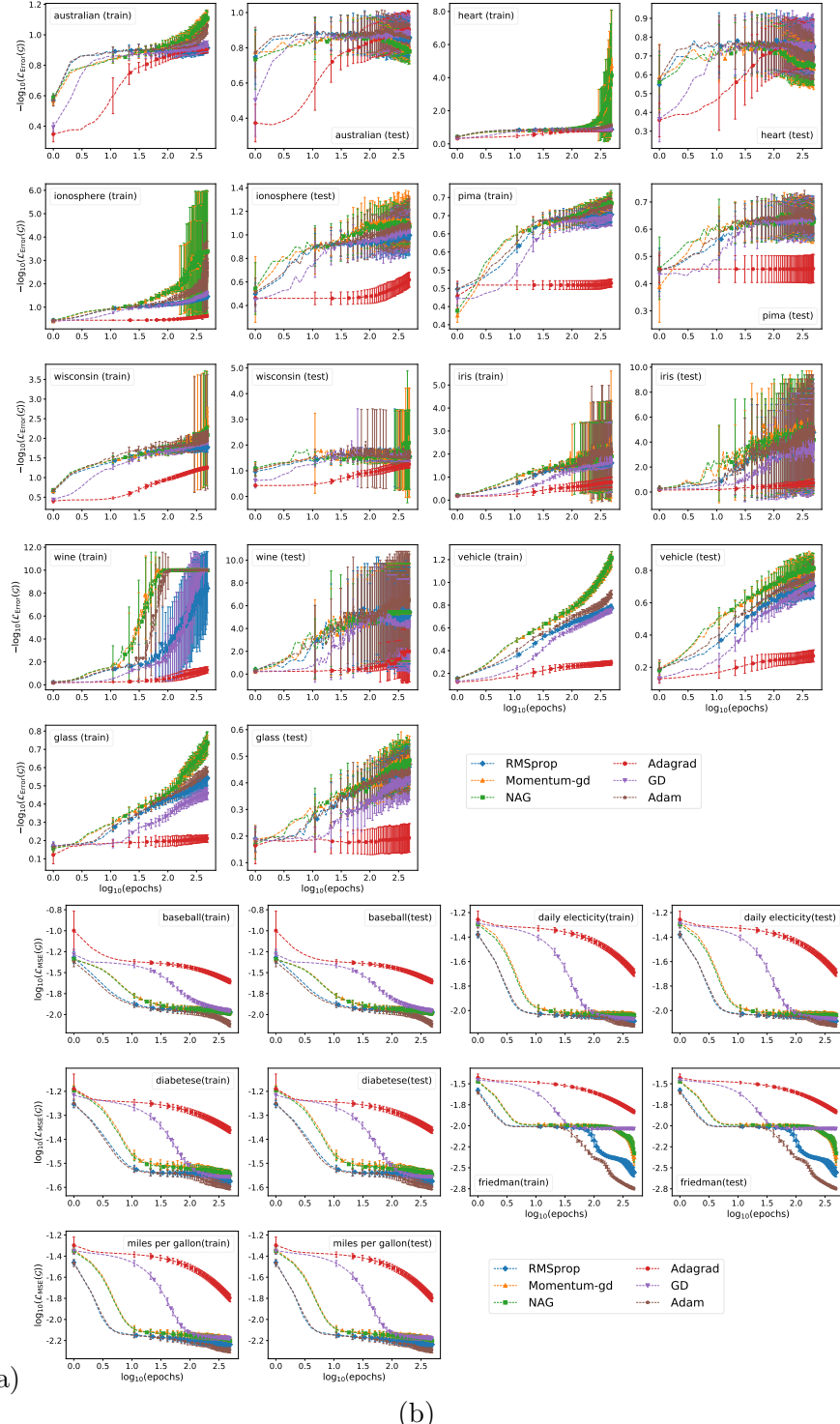


Fig. A7: MLP (a) classification (b) regression with *sigmoid* nodes trained with *default* learning rate and without an *early-stopping* strategy. (a) Adam and NAG in brown and green in this setting show more fluctuation as lines are on the upper side of plots. (b) Adam, RMSprop, and NAG in brown, blue, and green show better performance as lines are lower in plots.

1 A.3 Supplementary Tables

Table A1: Hyperparameter definition and choices used during the experiments of the algorithms. BNeuralT and MLP parameters setting are listed in detail. Some of the basic settings as recommended in the library or literature of HFNT, DT/RF, GP, NCB, and SVM are listed in this table.

Parameter	Definition	Default Rang	Choices used
BNeuralT	Scaling	Input-features scaling range.	$[min, max]$, [0, 1]
	Tree height	Maximum depth (layers) of a tree model.	$\{p \in \mathbb{Z} > 1\}$ {5, 10}
	Tree arity	Maximum arguments of a node m .	$\{m \in \mathbb{Z} \geq 2\}$ {5, 10}
	Tree edge	Initialization of neural weights of tree	$[w_l, w_u]$, $w_l \in \mathbb{R}$, $w_u \in \mathbb{R}$ [0, 1]
	$P[\text{leaf}_p < p]$	Leaf generation at depth $< p$	$P[\text{leaf}_p < p] \in [0, 1]$ {0.4, 0.5}
	Internal nodes	An activation function	{Sigmoid, ReLU, tanh} {Sigmoid, ReLU}
MLP	Layers	Number of hidden layers in architecture	1
	Hidden nodes	Number of nodes at hidden layer	100
	Activation nodes	An activation function	{Sigmoid, ReLU, tanh} {Sigmoid, ReLU}
Optimizers	Learning rate	Optimizer's learning rate	$\eta \in [0, 1]$ {0.1, 0.01, 0.001}
	Momentum rate	Optimizers momentum rate	$\gamma \in [0, 1]$ {0.9}
	Training epochs	Condition for algorithm termination	$\{Epochs \in \mathbb{Z} > 1\}$ 500
	Early-stopping	Stopping algorithm to avoid overfitting	$[0, Epochs]$ {50}
	Algorithms	Method of early-stopping	Fallback $\in [\text{True}, \text{False}]$ True
		Algorithms for optimization	{GD, MGD, NAG, Adagrad, RMSprop, Adam, L-BFGS (Liu and Nocedal, 1989)}
HFNT	Tree setup	Height = 10, arity = 5, edge = [0, 1], leaf generation is attribute dependent	
	Internal node	Takes arbitrarily any function from {Gaussian, Sigmoid, tanh, fermi, etc.}	
	Structure	Single and multi objective genetic programming with 50 population and 500 generations	
	Parameter	Differential evaluation with 100 population and 1000 generations, 0.9 crossover rate	
DT/RF	Tree depth	Restriction max depth of the tree	$\{p \in \mathbb{Z} > 1\}$ Unbounded
	Max leaf node	Restriction on max leaf node of a tree	Unbounded
	Split	Strategy for splitting a decision node	“best”
	Criteria	Decision criteria about an input	Classification “gini index” Regression MSE
GP	Random forest	Data sampling method for tree generation	bootstrap
	Estimators	The number of trees in the forest	100
GP	Optimizer	Algorithm used for kernel optimization	L-BFGS
	Training iteration	Condition for algorithm termination	$\{Epochs \in \mathbb{Z} > 1\}$ 100
	Classification	Method of multi-class classification	{1 vs rest, 1 vs 1} {1 vs rest}
	Kernel	Gaussian kernel used for learning	Classification radial basis Regression dot product + white noise
			radial basis {1 vs rest} L1 hinge loss
SVM	Kernel	Kernel used for learning	radial basis
	Classification	Method of multi-class classification	{1 vs rest, 1 vs 1 } {1 vs rest}
	Penalty	Regularization to avoid overfitting	L1
	Training loss	Loss function used during training	hinge loss
	Training iteration	Condition for algorithm termination	$\{Epochs \in \mathbb{Z} > 1\}$ 1000
NBC		It uses Gaussian function	

Table A2: Summary of top (based on overall performance) 55 of 110 experiments on all data, on all algorithms, and all settings . The values are an average of 30 independent runs of each setting. Names of experiments start with B indicate BNeuralIT and M indicate MLP. The next letter is S or R indicates sigmoid and ReLU activation function, ESy indicates early-stopping and ESn indicates no early-stopping, Rn or Ry indicates no regularization or elastic net regularization; L indicates default learning rate or absence of L indicates a learning rate of 0.1, Dr indicates dropout; p4 or p5 indicates leaf generation rate 0.4 or 0.5, and optimizers GD, MGD, NAG, Adagrad, RMSprop, and Adam are indicated with G, M, N, A, R, D, respectively.

Overall	Acc	σ_{Acc}	w	Classification	r_2	σ	w	Regression	Acc	σ_{Acc}	w
B-S-ESy-p4-R	.832	.15	222	B-S-ESy-p4-R	.891	.10	261	M-S-ESy-Rn-N	.775	.16	1041
M-S-ESy-Rn-N	.832	.14	1638	B-S-ESy-p5-R	.888	.11	157	M-S-ESy-Rn-L-D	.772	.16	1041
M-S-ESy-Rn-L-D	.831	.14	1638	B-S-ESy-p4-N	.875	.11	261	M-R-ESn-Rn-L-G	.761	.17	1041
M-S-ESy-Rn-G	.823	.14	1638	B-S-ESy-p4-M	.874	.11	261	M-S-ESy-Rn-M	.759	.22	1041
M-S-ESy-Rn-M	.822	.17	1638	B-S-ESy-p5-N	.871	.11	157	M-S-ESn-Rn-L-Dr-D	.754	.15	1041
<i>M-S-ESn-Rn-L-Dr-D</i>	.821	.14	1638	B-S-ESy-p5-M	.871	.11	157	M-S-ESy-Rn-L-R	.752	.16	1041
M-S-ESy-Rn-L-M	.821	.14	1638	GP	.868	.10		M-S-ESn-Rn-L-D	.749	.19	1041
M-S-ESy-Rn-L-N	.820	.14	1638	M-S-ESy-Rn-L-M	.868	.12	1970	M-S-ESn-Rn-L-R	.745	.17	1041
RF	.818	.14		M-S-ESy-Rn-L-N	.868	.11	1970	M-S-ESy-Rn-G	.744	.14	1041
M-S-ESy-Rn-L-R	.818	.14	1638	M-S-ESy-Rn-G	.867	.12	1970	M-S-ESy-Rn-L-M	.737	.14	1041
M-S-ESn-Rn-L-D	.817	.15	1638	M-S-ESy-Rn-L-Dr-N	.865	.12	1970	M-S-ESn-Rn-L-Dr-R	.737	.15	1041
M-S-ESn-Rn-L-R	.815	.14	1638	M-S-ESy-Rn-N	.865	.12	1970	M-S-ESy-Rn-A	.736	.14	1041
M-S-ESy-Rn-A	.814	.14	1638	RF	.864	.10		M-S-ESn-Rn-G	.735	.16	1041
M-S-ESy-Rn-L-Dr-D	.813	.14	1638	M-S-ESy-Rn-L-D	.863	.12	1970	RF	.735	.17	
B-S-ESy-p5-R	.812	.18	131	M-S-ESy-Rn-L-Dr-M	.863	.13	1970	M-S-ESy-Rn-L-N	.733	.14	1041
M-S-ESn-Rn-G	.812	.14	1638	M-S-ESn-Rn-L-Dr-M	.861	.11	1970	M-S-ESn-Rn-M	.733	.20	1041
M-S-ESn-Rn-A	.811	.14	1638	M-S-ESy-Rn-L-Dr-D	.861	.12	1970	SVM	.733	.20	
B-S-ESy-p4-N	.808	.17	222	M-S-ESn-Rn-L-Dr-D	.859	.11	1970	B-S-ESy-p4-R	.727	.17	152
M-S-ESn-Rn-L-Dr-R	.808	.14	1638	M-S-ESn-Rn-Dr-G	.860	.11	1970	M-S-ESn-Rn-A	.727	.14	1041
M-S-ESy-Rn-L-Dr-N	.808	.15	1638	M-S-ESn-Rn-L-Dr-N	.858	.11	1970	M-S-ESy-Rn-L-Dr-D	.725	.14	1041
M-S-ESn-Rn-L-N	.808	.15	1638	M-R-ESn-Rn-A	.858	.11	1970	M-S-ESn-Rn-L-M	.725	.17	1041
M-S-ESn-Rn-Dr-A	.807	.14	1638	M-S-ESy-Rn-Dr-G	.858	.13	1970	M-S-ESn-Rn-L-N	.724	.17	1041
B-S-ESy-p4-M	.807	.17	222	M-S-ESn-Rn-A	.857	.11	1970	M-S-ESn-Rn-Dr-N	.721	.16	1041
M-S-ESn-Rn-L-Dr-M	.807	.14	1638	M-S-ESy-Rn-A	.857	.12	1970	M-S-ESn-Rn-Dr-A	.719	.14	1041
M-S-ESn-Rn-L-M	.807	.15	1638	M-S-ESy-Rn-M	.857	.13	1970	M-S-ESn-Rn-N	.717	.26	1041
M-S-ESy-Rn-L-Dr-M	.807	.15	1638	M-S-ESn-Rn-Dr-A	.857	.12	1970	M-S-ESy-Rn-L-Dr-R	.717	.14	1041
GP	.806	.14		M-S-ESn-Rn-L-D	.856	.11	1970	M-S-ESy-Rn-L-G	.716	.14	1041
M-S-ESn-Rn-L-Dr-N	.805	.14	1638	M-S-ESn-Rn-G	.854	.11	1970	M-S-ESy-Rn-Dr-A	.715	.14	1041
M-S-ESy-Rn-L-G	.805	.14	1638	M-S-ESy-Rn-Dr-A	.854	.12	1970	M-S-ESn-Rn-L-Dr-N	.710	.14	1041
M-S-ESy-Rn-Dr-G	.805	.15	1638	M-S-ESn-Rn-L-N	.854	.11	1970	M-S-ESn-Rn-L-Dr-M	.709	.14	1041
M-S-ESy-Rn-Dr-A	.804	.14	1638	M-S-ESn-Rn-L-R	.854	.11	1970	B-S-ESy-p4-A	.708	.19	152
M-S-ESn-Rn-Dr-G	.804	.15	1638	M-S-ESy-Rn-L-G	.854	.12	1970	M-S-ESy-Rn-Dr-G	.708	.14	1041
SVM	.802	.16		M-S-ESy-Rn-L-R	.854	.12	1970	M-S-ESn-Rn-L-G	.707	.14	1041
M-S-ESy-Rn-L-Dr-R	.801	.14	1638	M-S-ESn-Rn-L-M	.852	.11	1970	M-S-ESy-Rn-L-Dr-M	.705	.14	1041
M-R-ESn-Rn-A	.801	.19	1638	B-S-ESy-p4-A	.852	.13	261	M-R-ESn-Rn-G	.704	.24	1041
B-S-ESy-p4-A	.801	.17	222	M-S-ESn-Rn-L-G	.852	.12	1970	M-S-ESn-Rn-Dr-G	.704	.14	1041
M-S-ESn-Rn-L-G	.800	.15	1638	M-S-ESy-Rn-R	.850	.15	1970	M-R-ESn-Rn-L-M	.704	.25	1041
M-R-ESn-Rn-L-G	.799	.14	1569	M-R-ESn-Rn-G	.850	.11	1970	M-S-ESy-Rn-L-Dr-N	.703	.14	1041
M-R-ESn-Rn-G	.798	.18	1638	M-S-ESy-Rn-L-Dr-R	.848	.13	1970	M-R-ESn-Rn-A	.698	.25	1041
B-S-ESy-p5-N	.790	.19	131	M-S-ESn-Rn-L-Dr-R	.848	.12	1970	M-R-ESn-Rn-L-N	.698	.26	1041
B-S-ESy-p5-M	.789	.19	131	B-S-ESy-p4-D	.843	.14	261	GP	.695	.13	
NBC	.782			M-S-ESn-Rn-L-Dr-G	.842	.13	1970	B-S-ESy-p5-L-R	.688	.19	95
M-S-ESn-Rn-L-Dr-G	.779	.16	1638	M-S-ESy-Rn-L-Dr-G	.842	.14	1970	B-S-ESy-p4-M	.687	.20	152
B-S-ESy-p5-A	.778	.19	131	SVM	.841	.13		M-R-ESn-Rn-L-A	.686	.16	1041
M-S-ESy-Rn-L-Dr-G	.777	.17	1638	B-S-ESy-p5-A	.841	.13	157	B-S-ESy-p4-N	.686	.20	152
B-S-ESy-p5-L-R	.776	.17	138	M-S-ESn-Rn-Dr-R	.841	.12	1970	B-S-ESy-p5-R	.676	.21	85
M-S-ESn-Rn-M	.770	.18	1638	B-S-ESy-p5-D	.840	.14	157	M-R-ESn-Rn-L-R	.675	.26	1041
M-R-ESn-Rn-L-M	.769	.19	1569	M-S-ESn-Rn-R	.838	.12	1970	B-S-ESy-p5-L-D	.673	.21	95
M-S-ESn-Rn-N	.769	.20	1638	B-S-ESy-p4-G	.832	.14	261	B-S-ESn-A	.668	.21	80
M-R-ESn-Rn-L-N	.767	.19	1569	M-S-ESy-Rn-Dr-R	.832	.14	1970	M-S-ESn-Rn-Dr-M	.667	.39	1041
B-S-ESn-A	.765	.19	128	B-S-ESn-R	.831	.12	154	M-S-ESn-Rn-L-Dr-G	.665	.14	1041
B-S-ESn-R	.765	.18	128	B-S-ESy-p5-G	.830	.14	157	B-S-ESy-p5-A	.664	.22	85
B-S-ESy-p4-D	.765	.20	222	B-S-ESy-p5-L-N	.829	.14	162	M-S-ESy-Rn-L-Dr-G	.660	.15	1041
M-R-ESn-Rn-L-R	.762	.20	1569	B-S-ESy-p5-L-M	.828	.14	162	M-R-ESn-Rn-M	.656	.29	1041
B-S-ESn-N	.760	.19	128	M-R-ESn-Rn-L-G	.826	.11	1946	B-S-ESn-N	.651	.22	80

Table A3: Summary of last (based on overall performance) 55 of 110 experiments on all data, on all algorithms, and all settings . The values are an average of 30 independent runs of each setting. Names of experiments start with B indicate BNeuralT and M indicate MLP. The next letter is S or R indicates sigmoid and ReLU activation function, ESy indicates early-stopping and ESn indicates no early-stopping, Rn or Ry indicates no regularization or elastic net regularization; L indicates default learning rate or absence of L indicates a learning rate of 0.1, Dr indicates dropout; p4 or p5 indicates leaf generation rate 0.4 or 0.5, and optimizers GD, MGD, NAG, Adagrad, RMSprop, and Adam are indicated with G, M, N, A, R, D, respectively.

Overall	Acc	σ_{Acc}	w	Classification	r_2	σ	w	Regression	Acc	σ_{Acc}	w
B-S-ESn-M	.759	.19	128	B-S-ESy-p5-L-R	.825	.15	162	M-R-ESn-Rn-N	.650	.30	1041
B-S-ESy-p5-L-D	.751	.19	138	M-R-ESn-Rn-L-R	.824	.10	1946	B-S-ESn-M	.649	.22	80
B-S-ESy-p4-G	.750	.21	222	M-S-ESy-Rn-D	.821	.15	1970	B-S-ESn-R	.646	.21	80
B-S-ESy-p5-D	.747	.21	131	B-S-ESn-N	.821	.13	154	B-S-ESy-p5-N	.644	.22	85
M-R-ESn-Rn-L-D	.747	.24	1569	M-R-ESn-Rn-L-D	.820	.11	1946	M-R-ESn-Rn-L-D	.644	.32	1041
M-S-ESn-Rn-Dr-N	.744	.17	1638	B-S-ESn-M	.820	.13	154	B-S-ESy-p5-M	.643	.22	85
B-S-ESy-p5-L-N	.740	.22	138	B-S-ESn-A	.819	.14	154	M-S-ESy-Rn-Dr-N	.628	.64	1041
B-S-ESy-p5-L-M	.740	.22	138	M-R-ESn-Rn-L-N	.817	.11	1946	B-S-ESy-p4-D	.623	.21	152
B-S-ESy-p5-G	.737	.22	131	B-R-ESy-p5-R	.817	.14	150	B-S-ESy-p4-G	.602	.23	152
M-S-ESy-Rn-Dr-N	.733	.41	1638	M-R-ESn-Rn-L-M	.816	.11	1946	B-S-ESn-G	.582	.24	80
M-R-ESn-Rn-L-A	.732	.16	1569	DT	.813	.11		B-S-ESy-p5-L-M	.580	.24	95
B-S-ESn-G	.720	.21	128	B-R-ESy-p5-G	.802	.18	150	B-S-ESy-p5-L-N	.580	.24	95
M-S-ESn-Rn-Dr-M	.714	.27	1638	M-S-ESn-Rn-N	.798	.15	1970	B-S-ESy-p5-D	.579	.21	85
HFNT ^S	.708	.32		B-S-ESn-G	.797	.14	154	B-S-ESy-p5-G	.570	.24	85
B-R-ESy-p5-A	.706	.22	125	B-R-ESy-p5-A	.795	.16	150	HFNT ^M	.567	.54	
B-S-ESn-D	.705	.21	128	B-S-ESy-p5-L-D	.795	.16	162	HFNT ^S	.562	.44	
HFNT ^M	.704	.37		M-S-ESn-Rn-D	.792	.15	1970	B-S-ESn-D	.557	.23	80
DT	.695	.27		M-S-ESy-Rn-Dr-N	.791	.17	1970	B-R-ESy-p5-A	.544	.24	81
B-R-ESy-p5-R	.689	.25	125	M-S-ESy-Rn-Dr-D	.791	.17	1970	B-R-ESy-p5-N	.484	.25	81
B-R-ESy-p5-G	.683	.32	125	M-S-ESn-Rn-M	.791	.17	1970	DT	.484	.34	
B-R-ESy-p5-N	.677	.24	125	M-S-ESy-Rn-Dr-M	.789	.16	1970	B-R-ESy-p5-M	.483	.25	81
B-R-ESy-p5-M	.676	.24	125	HFNT ^S	.789	.18		M-S-ESy-Rn-L-A	.482	.16	1041
M-S-ESn-Rn-L-A	.639	.22	1638	B-S-ESn-D	.788	.15	154	M-S-ESn-Rn-L-A	.479	.16	1041
M-S-ESy-Rn-L-A	.635	.22	1638	B-R-ESy-p5-N	.784	.16	150	B-R-ESy-p5-G	.470	.39	81
M-S-ESy-Rn-Dr-M	.622	.75	1638	B-R-ESy-p5-M	.782	.15	150	B-R-ESy-p5-R	.457	.23	81
B-S-ESy-p5-L-G	.602	.26	138	NBC	.782			B-S-ESy-p5-L-G	.394	.26	95
B-R-ESy-p5-D	.583	.28	125	HFNT ^M	.779	.18		B-R-ESy-p5-D	.358	.28	81
M-S-ESn-Rn-L-Dr-A	.569	.24	1638	M-S-ESn-Rn-Dr-D	.773	.18	1970	M-S-ESn-Rn-L-Dr-A	.342	.12	1041
M-S-ESy-Rn-L-Dr-A	.556	.25	1638	M-R-ESn-Rn-L-A	.764	.15	1946	M-S-ESy-Rn-Dr-M	.320	1.18	1041
M-R-ESn-Rn-M	.543	.23	1638	M-R-ESn-Rn-R	.760	.23	1970	M-S-ESy-Rn-L-Dr-A	.320	.15	1041
M-R-ESn-Rn-N	.527	.24	1638	M-S-ESn-Rn-Dr-N	.757	.17	1970	M-S-ESn-Ry-L-A	-0.016	.02	1041
M-S-ESn-Ry-L-G	.468	.42	1638	M-S-ESn-Ry-L-G	.743	.25	1970	M-S-ESn-Ry-A	-0.019	.03	1041
M-S-ESn-Ry-L-D	.442	.40	1638	M-S-ESn-Rn-Dr-M	.739	.17	1970	M-S-ESn-Ry-L-D	-0.025	.04	1041
M-S-ESn-Ry-A	.431	.39	1638	M-S-ESn-Rn-L-A	.728	.20	1970	M-S-ESn-Ry-L-G	-0.027	.04	1041
M-S-ESn-Ry-L-N	.429	.43	1638	M-S-ESy-Rn-L-A	.719	.20	1970	M-S-ESn-Ry-L-R	-0.040	.05	1041
M-S-ESn-Ry-L-M	.429	.41	1638	B-S-ESy-p5-L-G	.718	.18	162	M-S-ESn-Ry-L-M	-0.058	.08	1041
M-S-ESn-Ry-L-R	.426	.41	1638	M-S-ESn-Ry-L-N	.711	.24	1970	M-S-ESn-Ry-G	-0.074	.12	1041
M-S-ESn-Ry-G	.425	.42	1638	B-R-ESy-p5-D	.707	.18	150	M-S-ESn-Ry-L-N	-0.077	.10	1041
M-S-ESn-Ry-N	.337	.37	1638	M-S-ESn-Ry-G	.702	.23	1970	M-S-ESn-Ry-N	-0.081	.12	1041
M-S-ESn-Ry-L-A	.304	.27	1638	M-S-ESn-Ry-L-D	.701	.26	1970	M-S-ESn-Ry-M	-0.118	.28	1041
M-S-ESn-Ry-M	.274	.37	1638	M-S-ESn-Ry-L-M	.699	.24	1970	B-S-ESy-p5-L-A	-0.445	.85	95
M-S-ESy-Rn-Dr-R	.267	1.15	1638	M-S-ESn-Rn-L-Dr-A	.695	.19	1970	M-S-ESy-Rn-Dr-R	-0.748	1.44	1041
B-S-ESy-p5-L-A	.178	.70	138	M-S-ESy-Rn-L-Dr-A	.687	.20	1970	M-R-ESn-Rn-D	-1.338	4.05	1041
M-S-ESn-Rn-Dr-R	-0.027	1.82	1638	M-S-ESn-Ry-L-R	.684	.26	1970	M-S-ESn-Rn-Dr-R	-1.589	2.34	1041
M-R-ESn-Rn-D	-0.072	2.60	1638	M-S-ESn-Ry-A	.681	.26	1970	M-S-ESn-Rn-R	-2.096	4.00	1041
M-S-ESy-Rn-R	-0.208	2.89	1638	M-R-ESn-Rn-D	.631	.23	1970	M-S-ESy-Rn-R	-2.112	4.22	1041
M-S-ESn-Rn-R	-0.210	2.77	1638	M-S-ESn-Ry-N	.569	.23	1970	M-R-ESn-Rn-R	-2.750	4.03	1041
M-R-ESn-Rn-R	-0.494	2.94	1638	B-S-ESy-p5-L-A	.523	.18	162	M-S-ESn-Ry-R	-2.829	4.03	1041
M-S-ESy-Rn-Dr-D	-0.563	2.32	1638	M-S-ESn-Ry-R	.516	.20	1970	M-S-ESy-Rn-Dr-D	-3.000	2.41	1041
M-S-ESn-Ry-R	-0.679	2.89	1638	M-S-ESn-Ry-D	.511	.20	1970	M-S-ESn-Rn-Dr-D	-3.932	2.95	1041
M-S-ESn-Rn-Dr-D	-0.908	2.86	1638	M-S-ESn-Ry-M	.492	.20	1970	M-S-ESn-Ry-D	-4.080	2.99	1041
M-S-ESn-Rn-D	-0.983	3.05	1638	M-S-ESn-Ry-L-A	.481	.17	1970	M-S-ESn-Rn-D	-4.179	3.17	1041
M-S-ESy-Rn-D	-1.014	3.28	1638	M-R-ESn-Rn-M	.481	.16	1970	M-S-ESy-Rn-D	-4.316	3.64	1041
M-S-ESn-Ry-D	-1.129	2.84	1638	M-R-ESn-Rn-N	.459	.16	1970	NBC			

Table A4: Wilcoxon signed-rank test on two samples: BNeuralT’s RMSprop against all other algorithms for each data. The ‘stat,’ ‘pval,’ and ‘post,’ respectively indicate Wilcoxon signed-rank statistic, two-tailed p -value, and Bonferroni correction post hoc adjusted p -value. The values are marked in bold where the null hypothesis that BNeuralT’s RMSprop and other algorithms have no difference is rejected.

		Classification									Regression					
BNeuralT’s RMSprop vs.		Aus	Hrt	Ion	Pma	Wis	Irs	Win	Vhl	Gls	Bas	Dee	Dia	Frd	Mpg	
MLP	GD	stat	87.5	22	21	8	81	7	35	33	18	199	164	180	90	80
		pval	0	0	0	0	.01	0	0	0	0	.49	.16	.28	0	0
		post	.03	0	0	0	.05	0	.05	0	0	1	1	1	.03	.02
	MGD	stat	112	28	70	35	116	22	25	3	43	157	183	197	219	112
		pval	.01	0	0	0	.05	.01	.08	0	0	.12	.31	.47	.78	.01
		post	.13	0	.01	0	.47	.05	.81	0	0	1	1	1	1	.12
	NAG	stat	101	27	55	43	116	22	32	4	46	153	186	193	195	107
		pval	.01	0	0	0	.05	.01	.11	0	0	.10	.34	.42	.44	.01
		post	.07	0	0	0	.47	.05	1	0	0	.92	1	1	1	.09
	Adagrad	stat	83	22	0	0	0	0	0	0	0	2	0	2	39	0
Trees		pval	0	0	0	0	0	0	0	0	0	0	0	0	0	0
		post	.02	0	0	0	0	0	0	0	0	0	0	0	0	0
	RMSprop	stat	106	32	19	15	131	18	28	33	9	156	181	192	68	187
		pval	.01	0	0	0	.10	0	.21	0	0	.12	.29	.40	0	.35
		post	.09	0	0	0	1	.03	1	0	0	1	1	1	.01	1
	Adam	stat	123.5	27	19	37	155	18	24	9	34	145	198	203	0	199
		pval	.02	0	0	0	.27	0	.42	0	0	.07	.48	.54	0	.49
		post	.25	0	0	0	1	.03	1	0	0	.65	1	1	0	1
	$\mathcal{M}_{0.4}$ Adam	stat	103	57	41	35	126	0	29	22	17	173	117	210	129	175
		pval	.01	0	0	0	.05	0	.13	0	0	.22	.02	.64	.03	.24
		post	.10	0	0	0	.62	0	1	0	0	1	.21	1	.40	1
Other	HFNT ^S	stat	24	38	6	21	76	25	22	0	15	117	118		108	115
		pval	0	0	0	0	0	0	0	0	0	.02	.02		.01	.02
		post	0	0	0	0	.03	0	0	0	0	0	0	0	.01	0
	HFNT ^M	stat	4	2	5	55	19	19	0	4	140	110		82	97	
		pval	0	0	0	0	0	0	0	0	0	.06	.01		0	.01
		post	0	0	0	0	0	0	0	0	0	1	1	1	1	.12
	DT	stat	1	3	23	0	0	5.5	0	69	130	16	0	1	61	0
		pval	0	0	0	0	0	0	0	0	.10	0	0	0	0	0
		post	0	0	0	0	0	0	0	.01	.96	0	0	0	0	0
	RF	stat	46.50	7	92.50	1	20	0	42	191	96	225	201	144	30	226
		pval	0	0	.01	0	0	0	.02	.57	.03	.88	.52	.07	0	.89
		post	.01	0	.09	0	0	0	.21	1	.33	1	1	.06	0	1
GP	GP	stat	67	12	55	20.5	50	14	36.5	13	112	187	143	201	89	24
		pval	0	0	0	0	0	0	.09	0	.04	.35	.07	.52	0	0
		post	.01	0	0	0	.01	0	.93	0	.38	1	.59	1	.03	0
	NBC	stat	1	30	13.5	10.5	0	10	28	0	0					
		pval	0	0	0	0	0	0	.01	0	0					
		post	0	0	0	0	0	0	.11	0	0					
SVM	SVM	stat	36	21	5.5	4.5	67.5	4.5	37.5	145	6	194	228	97	0	175
		pval	0	0	0	0	.01	0	.03	.29	0	.43	.93	.01	0	.24
		post	0	0	0	0	.06	0	.30	1	0	1	1	.05	0	1

Table A5: T-test on two independent samples: BNeuralT’s RMSprop against all other algorithms for each data. The ‘stat,’ ‘pval,’ and ‘post,’ respectively indicate T-test statistic, two-tailed p -value, and Bonferroni correction post hoc adjusted p -value. The values are marked in bold where null hypothesis that BNeuralT’s RMSprop and other algorithms have the same expected (average) is rejected.

BNeuralT’s RMSprop vs.		Classification								Regression						
		Aus	Hrt	Ion	Pma	Wis	Irs	Win	Vhl	Gls	Bas	Dee	Dia	Frd	Mpg	
MLP	GD	stat	3.21	6.87	7.51	6.17	2.52	3.93	2.55	-5.39	7.02	-1.22	1.38	.47	1.42	2.70
		pval	0	0	0	0	.01	0	.01	0	0	.23	.17	.64	.16	.01
		post	.02	0	0	0	.14	0	.13	0	0	1	1	1	1	.08
	MGD	stat	2.71	6.32	4.17	4.91	1.81	2.62	.83	-9.34	5.06	-2	.97	.23	-0.91	1.80
		pval	.01	0	0	0	.08	.01	.41	0	0	.05	.33	.82	.37	.08
		post	.09	0	0	0	.75	.11	1	0	0	.45	1	1	1	.70
	NAG	stat	2.75	6.46	5.05	4.97	1.85	2.73	.97	-9.78	4.39	-2.01	.96	.28	-0.30	1.78
		pval	.01	0	0	0	.07	.01	.33	0	0	.05	.34	.78	.76	.08
		post	.08	0	0	0	.70	.08	1	0	0	.44	1	1	1	.73
	Adagrad	stat	3.19	7.20	21.12	17.67	11.11	10.42	5.91	22.99	21.80	9.96	21.73	12.93	7.34	22.47
Trees		pval	0	0	0	0	0	0	0	0	0	0	0	0	0	0
		post	.02	0	0	0	0	0	0	0	0	0	0	0	0	0
	RMSprop	stat	2.69	6.07	8.03	6.40	2.08	3.22	0	-5.13	6.90	-1.98	.95	.22	-2.89	.21
		pval	.01	0	0	0	.04	0	1	0	0	.05	.35	.83	.01	.83
		post	.09	0	0	0	.42	.02	1	0	0	.47	1	1	.05	1
	Adam	stat	2.44	6.39	6.73	4.81	.78	3.06	0	-7.10	5.15	-2.13	.66	.05	-6.04	-0.84
		pval	.02	0	0	0	.44	0	1	0	0	.04	.51	.96	0	.40
		post	.18	0	0	0	1	.03	1	0	0	.34	1	1	0	1
	$\mathcal{M}_{0.4}$ Adam	stat	2.88	4.65	5.20	5.23	2.12	4.75	.30	-6.24	6.90	-1.69	2.30	.31	.56	.55
		pval	.01	0	0	0	.04	0	.76	0	0	.10	.03	.76	.58	.59
		post	.07	0	0	0	.50	0	1	0	0	1	.30	1	1	1
Others	HFNT ^S	stat	5.31	5.26	9.07	6.75	3.72	3.84	5.84	11.80	8.14	2.51	2.67		1.41	2.79
		pval	0	0	0	0	0	0	0	0	0	.01	.01		.16	.01
		post	0	0	0	0	.01	0	0	0	0	0	0	.04	0	
	HFNT ^M	stat	4.69	8.97	7.44	7.97	5.04	4.39	5.46	15.45	9.42	2.09	2.59		2.03	2.70
		pval	0	0	0	0	0	0	0	0	0	.04	.01		.05	.01
		post	0	0	0	0	0	0	0	0	0	.59	1	1	1	.97
	DT	stat	10.88	10.20	7.25	12.41	10.59	6.40	9.79	3.87	2.04	6.36	11.20	14.34	3.10	7.24
		pval	0	0	0	0	0	0	0	0	.05	0	0	0	0	0
		post	0	0	0	0	0	0	0	0	.46	0	0	0	.03	0
	RF	stat	3.43	7.32	2.69	9.75	6.73	5.50	1.55	.44	-2.21	.07	.65	1.92	-3.43	-0.40
		pval	0	0	.01	0	0	0	.13	.66	.03	.94	.52	.06	0	.69
		post	.01	0	.12	0	0	0	1	1	.40	1	1	.02	0	1
Others	GP	stat	4.12	7.03	4.52	7.35	4.19	5.03	1.14	-8.37	2.17	.65	1.61	.32	1.86	7.32
		pval	0	0	0	0	0	0	.26	0	.03	.52	.11	.75	.07	0
		post	0	0	0	0	0	0	1	0	.34	1	1	1	.62	0
	NBC	stat	12.03	5.53	8.72	8.75	11.12	6.22	2.60	28.51	14.55					
		pval	0	0	0	0	0	0	.01	0	0					
		post	0	0	0	0	0	0	.12	0	0					
Others	SVM	stat	4.43	5.50	7.99	7.72	2.83	7.57	1.88	-1.15	8.85	.66	-0.08	3.27	-4.91	.63
		pval	0	0	0	0	.01	0	.06	.26	0	.51	.93	0	0	.53
		post	0	0	0	0	.06	0	.65	1	0	1	1	.02	0	1